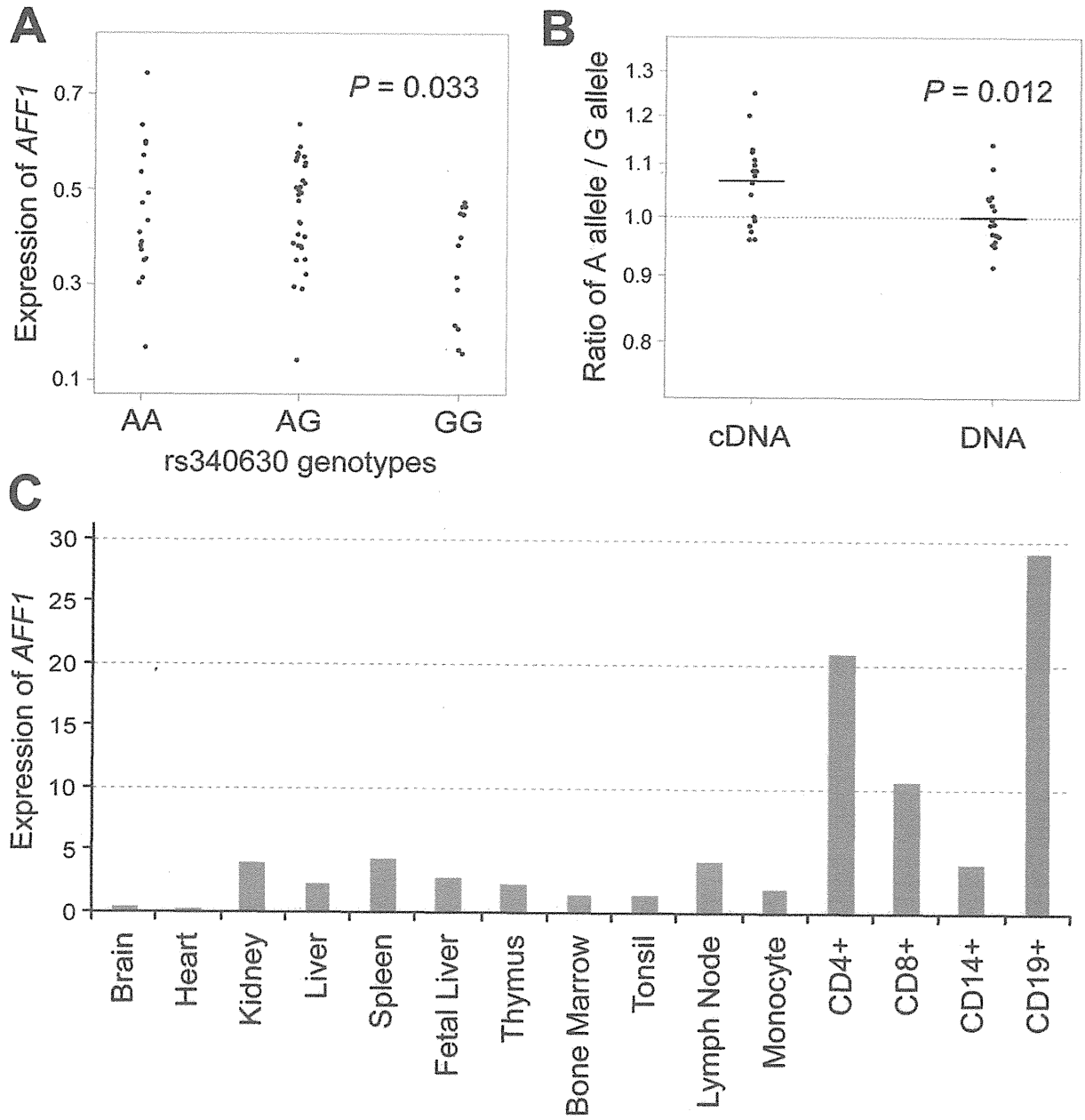

Figure 3. Association of rs340630 with *AFF1* expression. (A) Correlation between rs340630 genotypes and transcript levels of *AFF1* (NM_001166693) in EBV-transfected cell lines ($n = 62$) stimulated with PMA. (B) Allele-specific quantification (ASTQ) of *AFF1* transcripts. Allele specific-probes for rs340638 were used for quantification by qPCR. The ratios of A allele over G allele for the amounts of both cDNAs and DNAs were plotted in log scale for each cell line. (C) *AFF1* expression in various tissues. Transcripts levels of *AFF1* were quantified by qPCR and were normalized by *GAPDH* levels.
doi:10.1371/journal.pgen.1002455.g003

non-autosomal SNPs, and SNPs not shared between SLE cases and controls, were excluded. We excluded 7 closely related SLE cases in a 1st or 2nd degree of kinship based on identity-by-descent estimated using PLINK version 1.06 [41]. We then excluded 1 SLE cases and 1 controls whose ancestries were estimated to be distinct from East-Asian populations using PCA performed along with the genotype data of Phase II HapMap populations (release 24) [29] using EIGENSTRAT version 2.0 [42]. Subsequently, SNPs with minor allele frequencies <0.01 in SLE cases or controls, SNPs with exact *P*-values of Hardy-Weinberg equilibrium test $<1.0\times10^{-6}$ in controls, or SNPs with ambiguous cluster plots were excluded. Finally, 430,797 SNPs for 891 SLE cases and 3,384 controls were obtained. Genotyping of SNPs in replication studies was performed using TaqMan Assay or Illumina HumanHap610-Quad Genotyping BeadChip (Illumina, CA, USA).

Association analysis of the SNPs

Association of SNPs in GWAS and replication studies were tested with Cochran-Armitage's trend test. Combined analysis was performed with Mantel-Haenzel method. Associations of previously reported SLE susceptibility loci [3–18] were evaluated using the results of the GWAS. Genotype imputation was performed for non-genotyped SNPs using MACH version 1.0 [43] with Phase II HapMap East-Asian individuals as references [29], as previously described [44]. All imputed SNPs demonstrated imputation scores, *Rsq*, >0.70.

eQTL study

We analyzed gene expression data previously measured in lymphoblastoid B cell lines from Phase II HapMap East-Asian individuals using Illumina's human whole-genome expression array (WG-6 version 1) (accession number; GSE6536) [28]. Expression data were normalized across the individuals. We used BLAST to map 47,294 Illumina array probes onto human autosomal reference genome sequences (Build 36). We discarded probes mapped with expectation values smaller than 0.01 to multiple loci, or for which there was polymorphic HapMap SNP(s) inside the probe. Then, 19,047 probes with exact matches to a unique locus with 100% identity and with a mean signal intensity greater than background were obtained. Genotype data of HapMap individuals were obtained for SNPs included in the GWAS. Associations of SNP genotypes (coded as 0, 1, and 2) with expression levels of each of the cis-eQTL probes (located within ±300 kbp regions of the SNPs) were evaluated using linear regression assuming additive effects of the genotypes on the expression levels. Considering the significant overlap between eQTL and genetic loci responsible for autoimmune diseases [24], we applied relatively less stringent multiple testing threshold of FDR *Q*-values<0.2 for the definition of eQTL. SNPs that exhibited this threshold with any of the corresponding cis-eQTL probes were denoted as eQTL positive.

Selection of SNPs enrolled in the replication studies

In order to select SNPs for further replication studies, we firstly integrated the results of GWAS and eQTL study. SNPs that satisfied $P<1.0\times10^{-4}$ in GWAS, or the SNPs that satisfied $1.0\times10^{-4}\leq P<1.0\times10^{-3}$ in GWAS and denoted as eQTL positive, were selected. Among these, SNPs most significantly associated in each of the genomic loci and not included in the previously reported SLE susceptibility loci [3–18] were further evaluated.

Then, the results of the concurrently proceeding genome-wide scan for SLE in the Japanese subjects using a pooled DNA approach were referred (Tahira T et al. Presented at the 59th Annual Meeting of the American Society of Human Genetics, October 21, 2009). In the scan, DNA collected from 447 SLE cases and 680 controls of Japanese origin were pooled respectively, and genotyped using GeneChip Human Mapping 500K Array Set (Affymetrix, CA, USA). SNPs were ranked according to the Silhouette scores estimated based on relative allele scores (RAS) between SLE cases and controls, and rank-based *P*-values were assigned [30]. By referring to association signals in multiple neighboring SNPs in the pooled analysis, we selected SNPs for replication study 1. Namely, if the SNP of interest was in LD ($r^2>0.5$) or was located within ±100 kbp of SNPs showing association signals in the pooled analysis (rank-based $P<0.01$), it would be selected. SNPs that satisfied $P<1.0\times10^{-6}$ in the combined study of GWAS and replication study 1 were further evaluated in replication study 2 (Figure 1).

Quantification of *AFF1* expression

EBV-transformed lymphoblastoid cell lines ($n=62$) were established by Pharma SNP Consortium (Tokyo, Japan) using peripheral blood lymphocytes of Japanese healthy individuals. Cells were incubated for 2 h in medium alone (RPMI 1640 medium containing 10% FBS, 1% penicillin, and 1% streptomycin) or with 100 ng/ml PMA. Conditions for cell stimulation were optimized before the experiment as previously described [45]. Cells were then harvested and total RNA was isolated using an RNeasy Mini Kit (Qiagen) with DNase treatment. Total RNA (1 μg) was reverse transcribed using TaqMan Gold RT-PCR reagents with random hexamers (Applied Biosystems). Real-time quantitative PCR was performed in triplicate using an ABI PRISM 7900 and TaqMan gene expression assays (Applied Biosystems). Specific probes (Hs01089428_m1) for transcript of *AFF1* (NM_001166693) were used. Expression of *AFF1* in various tissues was also quantified using Premium Total RNA (Clontech). The data were normalized to *GAPDH* levels. *GUS* levels were also evaluated for internal control, and similar results were obtained. Correlation coefficient, R^2, between rs340630 genotypes and transcript levels of *AFF1* was evaluated.

Allele-specific transcript quantification (ASTQ)

ASTQ of *AFF1* in PSC cells was performed as previously described [46]. DNAs were extracted by using a DNeasy Kit (QIAGEN). RNA extraction and cDNA preparation were performed as described above. For PSC cells ($n=17$) that were heterozygous for both rs340630 (the landmark SNP of GWAS) and rs340638 (located in the 5′-untranslated region of *AFF1* and in absolute LD with rs340630), expression levels of *AFF1* were quantified by qPCR on an ABI Prism 7900 using a custom-made TaqMan MGB-probe set for rs340638. Primer sequences were 5′-CTAACTGTGGCCCGCGTTG-3′ and 5′-CCCGGCGCAGTTTCTGAG-3′. The probe sequences were 5′-VIC-CGAAGACCGCCAGCGCCCAAC-TAMRA-3′ and 5′-FAM-CGAAGACCGCCGGCGCCCAA-TAMRA-3′. Ct values of VIC and FAM were obtained for genomic DNA and cDNA samples after 40 cycles of real-time PCR. We also prepared genomic DNA of samples homozygous for each allele and mixed them at different ratios (2:8, 3:7, 4:6, 5:5, 6:4, 7:3, 8:2) to create a standard curve by plotting Ct values of VIC/FAM against the allelic ratio of VIC/FAM for each mixture. Using the standard curve, we calculated the allelic ratios for each genomic DNA and cDNA samples. We measured each sample in quadruplicate in one assay; tests were independently repeated twice.

Web resources

The URLs for data presented herein are as follows.

NCBI GEO, http://www.ncbi.nlm.nih.gov/geo

BioBank Japan Project, http://biobankjp.org

PLINK software, http://pngu.mgh.harvard.edu/~purcell/plink/index.shtml

International HapMap Project, http://www.hapmap.org

EIGENSTRAT software, http://genepath.med.harvard.edu/~reich/Software.htm

MACH and mach2qtl software, http://www.sph.umich.edu/csg/abecasis/MACH/index.html

SNAP, http://www.broadinstitute.org/mpg/snap/index.php

Supporting Information

Figure S1 Principal component analysis (PCA) plot of the subjects. PCA plot of subjects enrolled in the GWAS for SLE. SLE cases and the controls enrolled in the GWAS are plotted based on

eigenvectors 1 and 2 obtained from the PCA using EIGENSTRAT version 2.0 [42], along with European (CEU), African (YRI), Japanese (JPT), and Chinese (CHB) individuals obtained from the Phase II HapMap database (release 22) [29]. Subjects who were estimated to be outliers in terms of ancestry from East-Asian (JPT+CHB) clusters and excluded from the study are indicated by black arrows.
(TIF)

Figure S2 Quantile-Quantile plot (QQ-plot) of *P*-values in the GWAS for SLE. The horizontal axis indicates the expected $-\log_{10}$ (*P*-values). The vertical axis indicates the observed $-\log_{10}$ (*P*-values). The QQ-plot for the *P*-values of all SNPs that passed the quality control criteria is indicated in blue. The QQ-plot for the *P*-values after the removal of SNPs included in the previously reported SLE susceptibility loci is indicated in black. The gray line represents $y = x$. The SNPs for which the *P*-value was smaller than 1.0×10^{-15} are indicated at the upper limit of the plot.
(TIF)

Table S1 Basal characteristics of cohorts.
(DOC)

Table S2 Frequency of clinical characteristics of SLE in this GWAS.
(DOC)

Table S3 Distributions of eQTL positivity rates of the SNPs.
(DOC)

Table S4 Results of replication study 1 for Japanese patients with SLE.
(DOC)

Table S5 Results of replication studies 1 and 2 for Japanese patients with SLE.
(DOC)

Acknowledgments

We are grateful to Dr. A. Miyatake, the members of the Rotary Club of Osaka-Midosuji District 2660 Rotary International in Japan, the autoimmune disease study group, and the staffs of the BioBank Japan Project for supporting the study and clinical sample collection. We thank the members of the Laboratory for Autoimmune Diseases, CGM, RIKEN, for their assistance.

Author Contributions

Conceived and designed the experiments: Y. Okada, K. Shimane, Y. Kochi, A. Suzuki, M. Kubo, N. Kamatani, R. Yamada, Y. Nakamura, K. Yamamoto. Performed the experiments: Y. Kochi, N. Hosono, M. Kubo, K. Myouzen, T. Horiuchi, T. Tahira, K. Hayashi. Analyzed the data: Y. Okada, A. Takahashi, T. Tsunoda, K. Higasa, R. Yamada. Contributed reagents/materials/analysis tools: T. Horita, T. Atsumi, T. Koike, T. Ishii, A. Okamoto, K. Fujio, M. Hirakata, H. Amano, Y. Takasaki, Y. Kondo, S. Ito, T. Sumida, K. Takada, A. Mimori, K. Saito, Y. Tanaka, M. Kamachi, N. Nishimoto, Y. Kawaguchi, C. Terao, K. Ohmura, T. Mimori, F. Matsuda, O.W. Mohammed, K. Matsuda, K. Shimane, K. Ikari, H. Yamanaka. Wrote the paper: Y. Okada, K. Shimane, Y. Kochi, A. Suzuki, R. Yamada, K. Yamamoto.

References

1. Lipsky PE (2001) Systemic lupus erythematosus: an autoimmune disease of B cell hyperactivity. Nat Immunol 2: 764–766.
2. Sestak AL, Shaver TS, Moser KL, Neas BR, Harley JB (1999) Familial aggregation of lupus and autoimmunity in an unusual multiplex pedigree. J Rheumatol 26: 1495–1499.
3. Sigurdsson S, Nordmark G, Goring HH, Lindroos K, Wiman AC, et al. (2005) Polymorphisms in the tyrosine kinase 2 and interferon regulatory factor 5 genes are associated with systemic lupus erythematosus. Am J Hum Genet 76: 528–537.
4. Graham RR, Kozyrev SV, Baechler EC, Reddy MV, Plenge RM, et al. (2006) A common haplotype of interferon regulatory factor 5 (IRF5) regulates splicing and expression and is associated with increased risk of systemic lupus erythematosus. Nat Genet 38: 550–555.
5. Graham RR, Kyogoku C, Sigurdsson S, Vlasova IA, Davies LR, et al. (2007) Three functional variants of IFN regulatory factor 5 (IRF5) define risk and protective haplotypes for human lupus. Proc Natl Acad Sci U S A 104: 6758–6763.
6. Remmers EF, Plenge RM, Lee AT, Graham RR, Hom G, et al. (2007) STAT4 and the risk of rheumatoid arthritis and systemic lupus erythematosus. N Engl J Med 357: 977–986.
7. Cunninghame Graham DS, Graham RR, Manku H, Wong AK, Whittaker JC, et al. (2008) Polymorphism at the TNF superfamily gene TNFSF4 confers susceptibility to systemic lupus erythematosus. Nat Genet 40: 83–89.
8. Nath SK, Han S, Kim-Howard X, Kelly JA, Viswanathan P, et al. (2008) A nonsynonymous functional variant in integrin-alpha(M) (encoded by ITGAM) is associated with systemic lupus erythematosus. Nat Genet 40: 152–154.
9. Harley JB, Alarcon-Riquelme ME, Criswell LA, Jacob CO, Kimberly RP, et al. (2008) Genome-wide association scan in women with systemic lupus erythematosus identifies susceptibility variants in ITGAM, PXK, KIAA1542 and other loci. Nat Genet 40: 204–210.
10. Kozyrev SV, Abelson AK, Wojcik J, Zaghlool A, Linga Reddy MV, et al. (2008) Functional variants in the B-cell gene BANK1 are associated with systemic lupus erythematosus. Nat Genet 40: 211–216.
11. Hom G, Graham RR, Modrek B, Taylor KE, Ortmann W, et al. (2008) Association of systemic lupus erythematosus with C8orf13-BLK and ITGAM-ITGAX. N Engl J Med 358: 900–909.
12. Graham RR, Cotsapas C, Davies L, Hackett R, Lessard CJ, et al. (2008) Genetic variants near TNFAIP3 on 6q23 are associated with systemic lupus erythematosus. Nat Genet 40: 1059–1061.
13. Musone SL, Taylor KE, Lu TT, Nititham J, Ferreira RC, et al. (2008) Multiple polymorphisms in the TNFAIP3 region are independently associated with systemic lupus erythematosus. Nat Genet 40: 1062–1064.
14. Han JW, Zheng HF, Cui Y, Sun LD, Ye DQ, et al. (2009) Genome-wide association study in a Chinese Han population identifies nine new susceptibility loci for systemic lupus erythematosus. Nat Genet 41: 1234–1237.
15. Gateva V, Sandling JK, Hom G, Taylor KE, Chung SA, et al. (2009) A large-scale replication study identifies TNIP1, PRDM1, JAZF1, UHRF1BP1 and IL10 as risk loci for systemic lupus erythematosus. Nat Genet 41: 1228–1233.
16. Yang W, Shen N, Ye DQ, Liu Q, Zhang Y, et al. (2010) Genome-wide association study in Asian populations identifies variants in ETS1 and WDFY4 associated with systemic lupus erythematosus. PLoS Genet 6: e1000841. doi:10.1371/journal.pgen.1000841.
17. Lessard CJ, Adrianto I, Kelly JA, Kaufman KM, Grundahl KM, et al. (2011) Identification of a systemic lupus erythematosus susceptibility locus at 11p13 between PDHX and CD44 in a multiethnic study. Am J Hum Genet 88: 83–91.
18. Yang J, Yang W, Hirankarn N, Ye DQ, Zhang Y, et al. (2011) ELF1 is associated with systemic lupus erythematosus in Asian populations. Hum Mol Genet 20: 601–607.
19. Hopkinson ND, Doherty M, Powell RJ (1994) Clinical features and race-specific incidence/prevalence rates of systemic lupus erythematosus in a geographically complete cohort of patients. Ann Rheum Dis 53: 675–680.
20. Danchenko N, Satia JA, Anthony MS (2006) Epidemiology of systemic lupus erythematosus: a comparison of worldwide disease burden. Lupus 15: 308–318.
21. Yang J, Benyamin B, McEvoy BP, Gordon S, Henders AK, et al. (2010) Common SNPs explain a large proportion of the heritability for human height. Nat Genet 42: 565–569.
22. Raychaudhuri S, Plenge RM, Rossin EJ, Ng AC, Purcell SM, et al. (2009) Identifying relationships among genomic disease regions: predicting genes at pathogenic SNP associations and rare deletions. PLoS Genet 5: e1000534. doi:10.1371/journal.pgen.1000534.
23. Cantor RM, Lange K, Sinsheimer JS (2010) Prioritizing GWAS results: A review of statistical methods and recommendations for their application. Am J Hum Genet 86: 6–22.
24. Dubois PC, Trynka G, Franke L, Hunt KA, Romanos J, et al. (2010) Multiple common variants for celiac disease influencing immune gene expression. Nat Genet 42: 295–302.
25. Cookson W, Liang L, Abecasis G, Moffatt M, Lathrop M (2009) Mapping complex disease traits with global gene expression. Nat Rev Genet 10: 184–194.
26. Kochi Y, Okada Y, Suzuki A, Ikari K, Terao C, et al. (2010) A regulatory variant in CCR6 is associated with rheumatoid arthritis susceptibility. Nat Genet 42: 515–519.
27. Yamaguchi-Kabata Y, Nakazono K, Takahashi A, Saito S, Hosono N, et al. (2008) Japanese population structure, based on SNP genotypes from 7003 individuals compared to other ethnic groups: effects on population-based association studies. Am J Hum Genet 83: 445–456.
28. Stranger BE, Nica AC, Forrest MS, Dimas A, Bird CP, et al. (2007) Population genomics of human gene expression. Nat Genet 39: 1217–1224.
29. The International HapMap Consortium (2003) The International HapMap Project. Nature 426: 789–796.

30. Pearson JV, Huentelman MJ, Halperin RF, Tembe WD, Melquist S, et al. (2007) Identification of the genetic basis for complex disorders by use of pooling-based genomewide single-nucleotide-polymorphism association studies. Am J Hum Genet 80: 126–139.
31. Xia ZB, Popovic R, Chen J, Theisler C, Stuart T, et al. (2005) The MLL fusion gene, MLL-AF4, regulates cyclin-dependent kinase inhibitor CDKN1B (p27kip1) expression. Proc Natl Acad Sci U S A 102: 14028–14033.
32. Isnard P, Core N, Naquet P, Djabali M (2000) Altered lymphoid development in mice deficient for the mAF4 proto-oncogene. Blood 96: 705–710.
33. Schadt EE, Molony C, Chudin E, Hao K, Yang X, et al. (2008) Mapping the genetic architecture of gene expression in human liver. PLoS Biol 6: e107. doi:10.1371/journal.pbio.0060107.
34. Ernst J, Kheradpour P, Mikkelsen TS, Shoresh N, Ward LD, et al. (2011) Mapping and analysis of chromatin state dynamics in nine human cell types. Nature 473: 43–49.
35. Stahl EA, Raychaudhuri S, Remmers EF, Xie G, Eyre S, et al. (2010) Genome-wide association study meta-analysis identifies seven new rheumatoid arthritis risk loci. Nat Genet 42: 508–514.
36. Nakamura Y (2007) The BioBank Japan Project. Clin Adv Hematol Oncol 5: 696–697.
37. Hochberg MC (1997) Updating the American College of Rheumatology revised criteria for the classification of systemic lupus erythematosus. Arthritis Rheum 40: 1725.
38. Suzuki A, Yamada R, Kochi Y, Sawada T, Okada Y, et al. (2008) Functional SNPs in CD244 increase the risk of rheumatoid arthritis in a Japanese population. Nat Genet 40: 1224–1229.
39. Shimane K, Kochi Y, Horita T, Ikari K, Amano H, et al. (2010) The association of a nonsynonymous single-nucleotide polymorphism in TNFAIP3 with systemic lupus erythematosus and rheumatoid arthritis in the Japanese population. Arthritis Rheum 62: 574–579.
40. Myouzen K, Kochi Y, Shimane K, Fujio K, Okamura T, et al. (2010) Regulatory polymorphisms in EGR2 are associated with susceptibility to systemic lupus erythematosus. Hum Mol Genet 19: 2313–2320.
41. Purcell S, Neale B, Todd-Brown K, Thomas L, Ferreira MA, et al. (2007) PLINK: a tool set for whole-genome association and population-based linkage analyses. Am J Hum Genet 81: 559–575.
42. Price AL, Patterson NJ, Plenge RM, Weinblatt ME, Shadick NA, et al. (2006) Principal components analysis corrects for stratification in genome-wide association studies. Nat Genet 38: 904–909.
43. Li Y, Willer C, Sanna S, Abecasis G (2009) Genotype imputation. Annu Rev Genomics Hum Genet 10: 387–406.
44. Okada Y, Takahashi A, Ohmiya H, Kumasaka N, Kamatani Y, et al. (2011) Genome-wide association study for C-reactive protein levels identified pleiotropic associations in the IL6 locus. Hum Mol Genet 20: 1224–1231.
45. Aikawa Y, Yamamoto M, Yamamoto T, Morimoto K, Tanaka K (2002) An anti-rheumatic agent T-614 inhibits NF-kappaB activation in LPS- and TNF-alpha-stimulated THP-1 cells without interfering with IkappaBalpha degradation. Inflamm Res 51: 188–194.
46. Akamatsu S, Takata R, Ashikawa K, Hosono N, Kamatani N, et al. (2010) A functional variant in NKX3.1 associated with prostate cancer susceptibility down-regulates NKX3.1 expression. Hum Mol Genet 19: 4265–4272.
47. Johnson AD, Handsaker RE, Pulit SL, Nizzari MM, O'Donnell CJ, et al. (2008) SNAP: a web-based tool for identification and annotation of proxy SNPs using HapMap. Bioinformatics 24: 2938–2939.

THE JOURNAL OF BIOLOGICAL CHEMISTRY VOL. 286, NO. 17, pp. 14963–14971, April 29, 2011

Marked Induction of c-Maf Protein during Th17 Cell Differentiation and Its Implication in Memory Th Cell Development*

Received for publication, January 6, 2011, and in revised form, February 23, 2011 Published, JBC Papers in Press, March 14, 2011, DOI 10.1074/jbc.M111.218867

Kojiro Sato[‡1,2], Fumihiko Miyoshi[‡1], Kazuhiro Yokota[‡], Yasuto Araki[‡], Yu Asanuma[‡], Yuji Akiyama[‡], Keigyou Yoh[§], Satoru Takahashi[¶], Hiroyuki Aburatani[‖], and Toshihide Mimura[‡]

From the [‡]Department of Rheumatology and Applied Immunology, Faculty of Medicine, Saitama Medical University, Saitama 350-0495, Japan, [§]Pathophysiology of Renal Diseases, Doctoral Program in Clinical Sciences, and [¶]Department of Anatomy and Embryology, Graduate School of Comprehensive Human Sciences, University of Tsukuba, Ibaraki 305-8575, Japan, and the [‖]Department of Cancer Systems Biology, Laboratory for Systems Biology and Medicine, Research Center for Advanced Science and Technology, University of Tokyo, Tokyo 153-8904, Japan

Until recently, effector T helper (Th) cells have been classified into two subsets, Th1 and Th2 cells. Since the discovery of Th17 cells, which produce IL-17, much attention has been given to Th17 cells, mainly because they have been implicated in the pathogenesis of various inflammatory diseases. We have performed transcriptome analysis combined with factor analysis and revealed that the expression level of c-Maf, which is considered to be important for Th2 differentiation, increases significantly during the course of Th17 differentiation. The IL-23 receptor (IL-23R), which is important for Th17 cells, is among putative transcriptional targets of c-Maf. Interestingly, the analysis of c-Maf transgenic Th cells revealed that the overexpression of c-Maf did not lead to the acceleration of the early stage of Th17 differentiation but rather to the expansion of memory phenotype cells, particularly with Th1 and Th17 traits. Consistently, mouse wild-type memory Th cells expressed higher mRNA levels of c-Maf, IL-23R, IL-17, and IFN-γ than control cells; in contrast, *Maf*$^{-/-}$ memory Th cells expressed lower mRNA levels of those molecules. Thus, we propose that c-Maf is important for the development of memory Th cells, particularly memory Th17 cells and Th1 cells.

Acquired immune responses have been divided into two major categories according to the cytokine-production patterns of T helper (Th) cells. Th1 cells produce abundant IFN-γ and play important roles in cellular immune responses. On the other hand, Th2 cells produce various cytokines involved in humoral immunity, such as IL-4. It has been a predominant concept that a skewed balance of Th1/Th2 responses could lead to pathological conditions like autoimmune diseases. Recently, Th17 cells have been discovered as the third type of effector Th cells that produce large amounts of proinflammatory cytokine IL-17A (IL-17) but only minimal amounts of IFN-γ or IL-4 (1, 2). Th17 cells have been shown to play important roles in the pathogenesis of various inflammatory disease models previously considered to be Th1 diseases, such as collagen-induced arthritis and experimental autoimmune encephalomyelitis (3, 4). Thus, Th17 cells have been receiving considerable attention from the viewpoint of the pathological basis of human inflammatory diseases.

Initially, Th17 cells were believed to be differentiated in the presence of IL-23; however, it was thereafter reported that the differentiation factors for Th17 cells are actually TGF-β and IL-6 and that IL-23 is a proliferation factor in mice (5–7). On the other hand, the possibility has been raised that IL-23 is not a mere growth factor for Th17 cells but is important for the differentiation (8–10) and/or proper function (11) of these cells. Recently, TGF-β-independent but IL-23-, IL-6-, and IL-1β-dependent Th17 differentiation has been reported (12). These nonconventional Th17 cells may be more important than conventional TGF-dependent Th17 cells in inflammatory conditions such as experimental autoimmune encephalomyelitis.

In terms of the intracellular mechanisms of Th17 differentiation, Stat3 seems to play an essential role (13, 14). This is not surprising because Stat3 is activated by phosphorylation occurring downstream of IL-6 and IL-23 signaling. In 2006, RAR-related orphan receptor (ROR)[3]γt was reported to be a master regulator transcription factor for Th17 differentiation (15); it is a nuclear receptor the ligand of which is as yet unknown. Another nuclear receptor, RORα, was also implicated to function synergistically with RORγt in Th17 differentiation (16). The entire network of transcription factors in Th17 cells, however, remains to be elucidated. Thus, we first tried to shed light on the network and encountered the transcription factor c-Maf.

* This work was supported in part by grants-in-aid for Scientific Research from the Ministry of Education, Culture, Sports, Science, and Technology of Japan and grants from the Mochida Memorial Foundation for Medical and Pharmaceutical Research, the Naito Foundation, the Kanae Foundation for the Promotion of Medical Science, Uehara Memorial Foundation, and the Kato Memorial Bioscience Foundation.

[1] Both authors contributed equally to this work.

[2] To whom correspondence should be addressed: Morohongo 38, Moroyama, Iruma-gun, Saitama 350-0495, Japan. Tel.: 81-49-276-1462; Fax: 81-49-295-4849; Email: satok@saitama-med.ac.jp.

[3] The abbreviations used are: ROR, RAR-related orphan receptor; qRT-PCR, quantitative RT-PCR; FC, fold change; cRNA, complementary RNA; IL-23R, IL-23 receptor; luc, luciferase; MARE, Maf recognition element; Tg, transgenic.

EXPERIMENTAL PROCEDURES

Mice—C57BL/6 mice were purchased from CLEA Japan, Inc., and T cell-specific c-Maf Tg mice (under the control of the human CD2 promoter and locus control region) were described previously (17). All the mice were maintained under specific pathogen-free conditions. All animal experiments were performed with the approval of the Animal Study Committee of Saitama Medical University and conformed to relevant guidelines and laws.

Th1/2/17 Cell Differentiation in Vitro—Mouse naive Th cells were purified from mouse spleens using a magnetic sorter and microbeads (AutoMACS system and $CD4^+CD62L^+$ T Cell Isolation Kit II, Miltenyi Biotec). They were cultured in RPMI 1640 medium containing 10% FCS (culture medium) and stimulated with plate-bound anti-CD3 and anti-CD28 mAbs (1 μg/ml each) for 3 days. Th1 cells were cultured with 10 ng/ml IL-12 and 10 μg/ml anti-IL-4 mAb; Th2 cells with 10 ng/ml IL-4 and 10 μg/ml anti-IFN-γ mAb; and Th17 cells with 10 ng/ml each of IL-6 and IL-23, 3 ng/ml TGF-β and 10 μg/ml each of anti-IFN-γ and anti-IL-4 mAbs. All of the antibodies were purchased from BD Biosciences, and the cytokines were purchased from R&D Systems.

GeneChip Analysis—Total RNA was used for cDNA synthesis by reverse transcription followed by the synthesis of biotinylated cRNA through *in vitro* transcription. After cRNA fragmentation, we performed hybridization with a mouse A430 GeneChip (Affymetrix). The raw data were analyzed using Affymetrix Microarray Suite (version 5.0) and normalized.

qRT-PCR and ELISA—We performed qRT-PCR analysis using an ABI PRISM 7000 Sequence Detection System with TaqMan Gene Expression Assay probes. The GAPDH expression level was used as the internal control. As to the analysis of cytokine production of Th cells, the cells were stimulated with phorbol 12-myristate 13-acetate (40 ng/ml) and ionomycin (1 μg/ml) for 5 h in the culture medium. Then, RNA was extracted from the cells, and the supernatant was subjected to ELISA. The mouse IL-17 ELISA kit was from R&D Systems.

Intracellular Staining of Transcription Factors and Cytokines—Mouse Th cells differentiated *in vitro* were preincubated with an anti-mouse CD16/CD32 (Fcγ receptor) mAb for 15 min on ice to block nonspecific staining. The cells were then fixed and permeabilized with BD Cytofix/Cytoperm (BD Bioscience) and stained with the primary Abs (anti-c-Maf Ab, M-153; anti-GATA-3 Ab, HG3-31, Santa Cruz Biotechnology). They were then stained with appropriate secondary Abs conjugated with Alexa Fluor 488 (Invitrogen). For intracellular cytokine staining, Th cells were cultured in the culture medium in the presence of phorbol 12-myristate 13-acetate (40 ng/ml) and ionomycin (1 μg/ml) for 5 h. In the last 1 h, monensin (Golgistop) was added. The cells were then fixed and permeabilized with BD Cytofix/Cytoperm and intracellularly stained with anti-IFN-γ-FITC plus anti-IL-17-PE, or anti-IFN-γ-FITC plus anti-IL-4-PE Abs (all reagents were from BD Biosciences). Stained cells were analyzed by FACScan or FACSCanto (BD Biosciences).

Factor Analysis—Transcription factors whose expression levels (normalized signals) were higher than 100 under at least one of the Th cell differentiation conditions were selected. Forty-three probes (including overlapping probes for the same genes) were subjected to factor analysis using SPSS software (version 15.0). By the unweighted least-squares method, two principal factors were extracted, and, after rotation by the varimax method with Kaiser normalization, each gene was positioned on a plane defined by Factors 1 and 2 according to its factor loadings.

Luciferase Assay—To construct the reporter plasmid pTA-*Il23r*-luc, the mouse *Il23r* promoter region (-1440 to +110) was ligated in the NheI and XhoI gap of the pTA-luc plasmid (Clontech). The following primers were used for PCR: 5′-GCT AGC TGG AGG CAT TTC CTC AGC TG-3′ (sense) and 5′-CTC GAG CTC AGG AAT TAG GGT CTC CT-3′ (antisense). A deletion mutant of pTA-*Il23r*-luc, which lacks a putative Maf binding site (MARE-like element) was constructed as described previously (18). DNA transfection and luciferase assays were performed as described previously (19, 20). Briefly, the reporter plasmid was transfected along with a c-Maf expression vector (21), a GATA-3 expression vector (22), and/or the control vector pcDNA3.1 into HEK293T cells using FuGENE 6 (Roche Applied Science). After 24 h, the cells were harvested, and luciferase activity was measured.

Statistical Analyses—*Error bars* indicate S.D. Student's *t* test was used for statistical analyses (*, $p < 0.05$ and **, $p < 0.01$).

RESULTS

Transcriptome Analysis of Th1/2/17 Cells during Course of Their Differentiation—First, we obtained the basic profiles of Th1/2/17 cell differentiation. Mouse naive Th cells were sorted and cultured under Th1, Th2, and Th17 cell differentiation conditions, and harvested on days 1 and 3. We also harvested Th0 cells on day 1. RNA extracted from the cells was subjected to transcriptome analysis using GeneChip. The expression levels of genes encoding IFN-γ, IL-4, and IL-17, which are "signature" cytokines produced by Th1, Th2, and Th17 cells, respectively, were up-regulated significantly in each subset, indicating that the differentiation conditions were appropriate (Fig. 1*A*).

Factor Analysis of Transcription Factors—To focus on transcription factors that are specifically up-regulated during the course of Th1/2/17 differentiation, we selected transcription factor genes whose expression levels (signals) were >100 in at least one of the Th conditions that we examined. Then, we performed factor analysis using the seven sets of data (days 1 and 3 for Th1/2/17 cells and day 1 for Th0 cells). Two principal "Factors" were extracted, and each gene is plotted in the two-dimensional space defined by Factors 1 and 2, according to its factor loading (Fig. 1*B*). As expected, dots representing RORγ (one dot) and RORα (four dots, because four different probes are attributed to RORα in the chip we used) were closely located in this diagram and both were high in Factor 2 but not in Factor 1. Interestingly, all the dots representing c-Maf were plotted nearest to the dot representing *Rorc*, suggesting that c-Maf is even more closely related to RORγ than RORα is to RORγ. Histograms of the GeneChip data of *Maf*, *Rorc*, and *Rora* are shown in Fig. 1*C*. Consistent with Fig. 1*B*, *Maf* and *Rorc* demonstrated a more Th17-specific expression pattern than *Rora*.

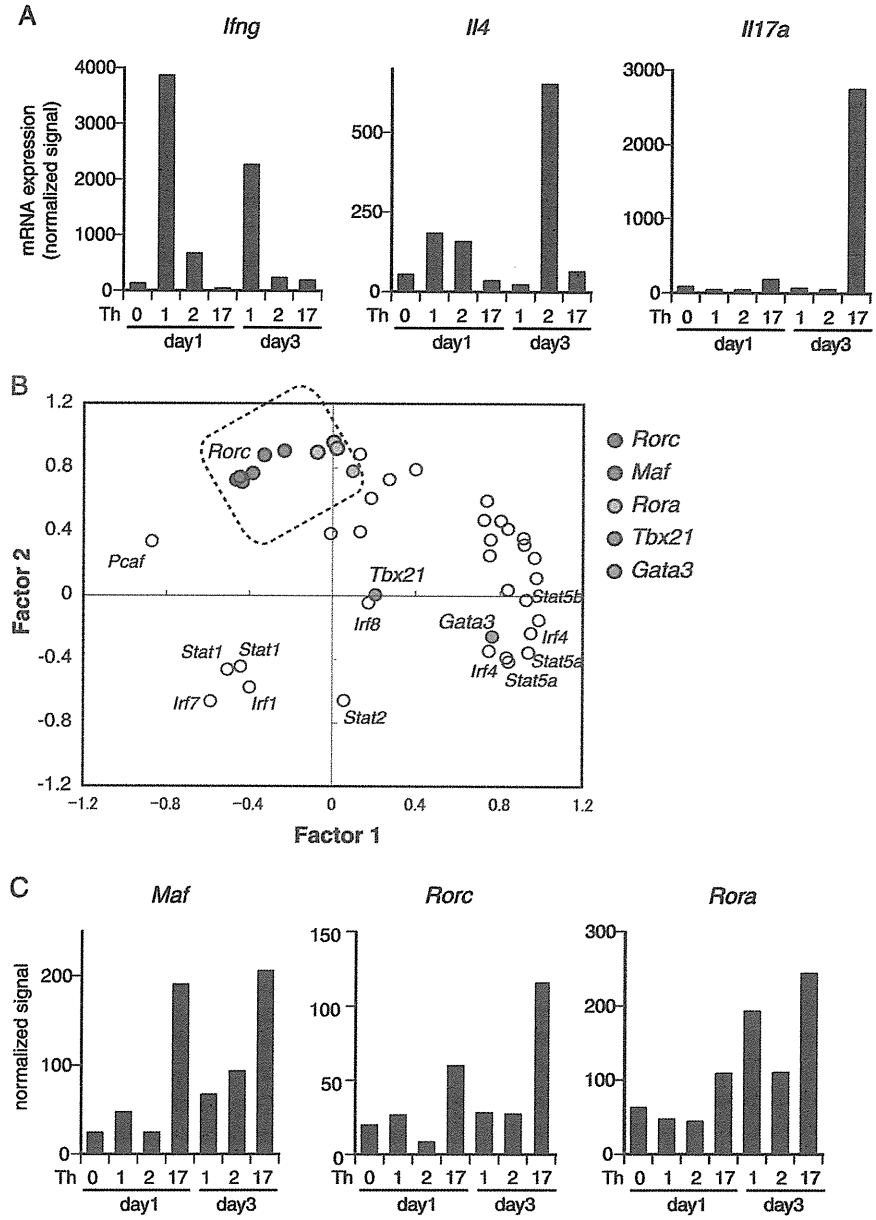

FIGURE 1. **Time series transcriptome analysis of genes representative of Th subsets at the mRNA level and factor analysis.** *A*, total RNA was obtained from Th cells cultured under the Th0, Th1, Th2, or Th17 conditions for 1 day (24 h) or 3 days (72 h). It was subjected to GeneChip analysis. As expected, IFN-γ, IL-4, and IL-17, the representative cytokines released from each Th subset, were induced in the relevant Th cells. *B*, distribution of transcription factors in a two-dimensional space defined by two factors extracted by factor analysis. Forty-three probes (including probes allotted to the same genes) were positioned in a plane defined by Factors 1 and 2. Note that all the probes representing RORγ, c-Maf, and RORα reside within a *box* with *dotted lines*. *C*, time series GeneChip data of *Maf* (data of one representative probe of five independent probes) and the known master regulator transcription factors for Th17 differentiation, namely, *Rorc* and *Rora* (data of one representative probe of four probes).

Expression of c-Maf but Not GATA-3 in Th17 Cells—The above data were rather unexpected in that c-Maf was reported to play important roles in Th2 differentiation (23). If c-Maf is highly expressed in Th17 cells, the question arises as to why they do not become Th2 cells. Indeed, similar levels of c-Maf protein expression were observed in the cells cultured under the Th2 and Th17 conditions (Fig. 2*A*, *left panel*). Interestingly, there was a large difference in GATA-3 expression level between the two subsets, whereas GATA-3 was barely detected in Th17 cells (Fig. 2*A*, *right panel*). This finding may explain why Th17 cells do not become Th2 cells. Indeed, IL-6 induces c-Maf by activating Stat3, which directly binds to the *Maf* promoter (24). GATA-3 is induced by IL-6, as well, but more indirect mechanisms are implicated (24). On the other hand, TGF-β, another important cytokine for the differentiation of mouse Th17 cells, is a potent inhibitor of Th2 development and has been shown to down-regulate GATA-3 (25). We added these cytokines to naive $CD4^+$ T cells separately or in combination and quantified the expression levels of two established markers of Th17 cells, IL-17 and IL-23R, in the screening for putative transcriptional targets of c-Maf. IL-6 alone induced *Il23r* but

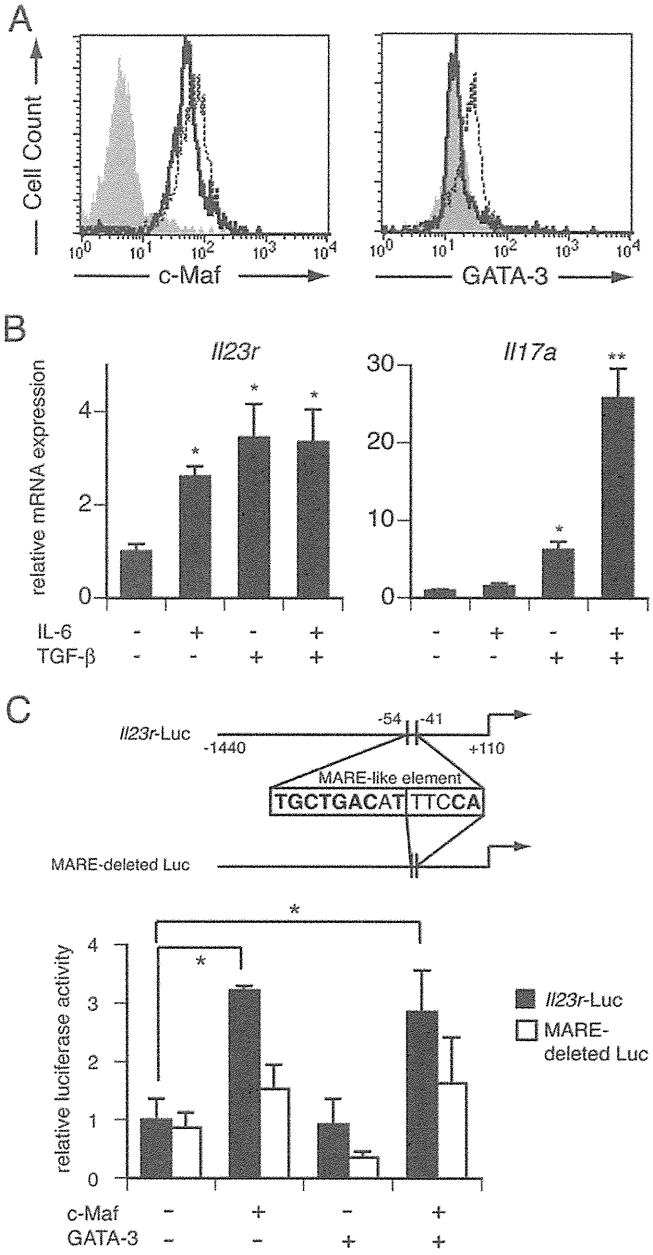

FIGURE 2. **Distinct expression patterns of c-Maf and GATA-3 in Th2 and Th17 cells and effects of these molecules on *Il23r* promoter.** *A*, flow cytometry analysis of c-Maf and GATA-3 expression in Th2 and Th17 cells. Although c-Maf expression was detected in both Th2 (*dotted line*) and Th17 (*solid line*) cells, GATA-3 expression was restricted to only Th2 cells. The *shaded areas* represent unstained Th2 cells (negative staining). *B*, qRT-PCR analysis of *Il23r* and *Il17a* expressions in naive $CD4^+$ T cells cultured for 3 days in the presence or absence of 10 ng/ml IL-6 and 3 ng/ml TGF-β. Anti-IFN-γ Ab and anti-IL-4 Ab (10 μg/ml each) were added to the culture. Either IL-6 or TGF-β is necessary for *Il23r* expression, but both cytokines are evidently necessary for significant *Il17a* induction. *C*, promoter analysis of *Il23r*. The 5′-flanking region of *Il23r* has a MARE-like sequence. (*Boldface letters* in the *box* correspond to MARE consensus sequences.) The forced expression of c-Maf had a positive effect on promoter activity, but that of GATA-3 did not. Furthermore, c-Maf did not significantly induce the luciferase activity of the deletion mutant lacking the MARE-like element, suggesting that c-Maf directly binds to this site. Data represent three independent experiments. *, $p < 0.05$.

it induced *Il17a* only slightly (Fig. 2*B*). Thus, *Il23r* is a candidate gene positively regulated by c-Maf.

Promoter Analysis of Putative c-Maf Target Genes—To obtain further insight, we performed luciferase promoter analysis using the promoters of the two genes. c-Maf overexpression induced the promoter activity of *Il23r*. c-Maf binds to a sequence called the Maf recognition element (MARE) (26). Indeed, the promoter region of *Il23r* contained a MARE-like sequence, and the deletion mutant luciferase vector that lacks the element lost responsiveness to c-Maf (Fig. 2*C*). Thus, c-Maf likely regulates Th17 proliferation via IL-23R induction. On the other hand, an ~1500-bp 5′ flanking region of *Il17a* responded to neither c-Maf nor GATA-3, suggesting that IL-17 is not a direct target of these factors (data not shown).

Ex Vivo Analysis of c-Maf Transgenic Mice—To confirm the hypothesis that c-Maf plays important role(s) in Th17 differentiation, we employed T cell-specific c-Maf Tg mice (17). As expected, the expression of IL-23R and IL-17 at the mRNA level was highly up-regulated in Tg Th cells. The expression of IFN-γ was also significantly up-regulated in Tg Th cells, but that of IL-4 was not (Fig. 3*A*). Flow cytometric analysis confirmed that the numbers of both IFN-γ-positive cells and IL-17-positive cells, but not that of IL-4-positive cells, were increased among Tg Th cells (Fig. 3*B*). To our surprise, although c-Maf Tg Th cells produced significantly more IL-17 than control cells *in vitro*, this difference disappeared when naive Th cells were sorted and stimulated under the same condition (Fig. 3*C*). This unexpected finding seems to be derived from the fact that most of the c-Maf Tg Th cells from the spleen demonstrate an effector-memory phenotype ($CD62L^{low}$ $CD44^{high}$, Fig. 3*D*). These results suggest that c-Maf does not play an essential role in the early differentiation of Th17 cells but rather in the development and/or maintenance of memory Th cells.

Analysis of WT Memory Phenotype Th Cells—The above findings on Tg Th cells prompted us to analyze WT memory Th cells. Under specific pathogen-free conditions, nearly 80% of the Th cells from the spleens of WT mice demonstrated the naive phenotype ($CD62L^{high}$ $CD44^{low}$, Fig. 4*A*, *left panel*). To facilitate the analysis of memory phenotype WT Th cells, we utilized the system of homeostatic expansion; when naive T cells are transferred into lymphopenic mice, they proliferate vigorously and acquire the memory phenotype (27). Thus, we transferred WT Th cells into Rag-2-deficient mice. In 4 weeks, most of the splenic Th cells from the recipient mice acquired an effector-memory phenotype ($CD62L^{low}$ $CD44^{high}$, Fig. 4*A*, *right panel*). When compared with WT naive Th cells, these cells expressed significantly higher mRNA levels of *Maf* and *Il23r* (Fig. 4*B*). Similar to the results in Fig. 3, these cells also expressed higher levels of *Il17a* and *Ifng* mRNAs, but not *Il4* mRNA (Fig. 4*C*). Consistent with the data, flow cytometric analysis revealed more IFN-γ-positive and IL-17-positive cells than WT naive cells (Fig. 4*D* and data not shown). Interestingly, an IFN-γ/IL-17 double-positive population was evident (IL-17 single-positive cells and IFN-γ/IL-17 double-positive cells were present at similar levels). On the other hand, IL-4-positive cells were scarcely observed.

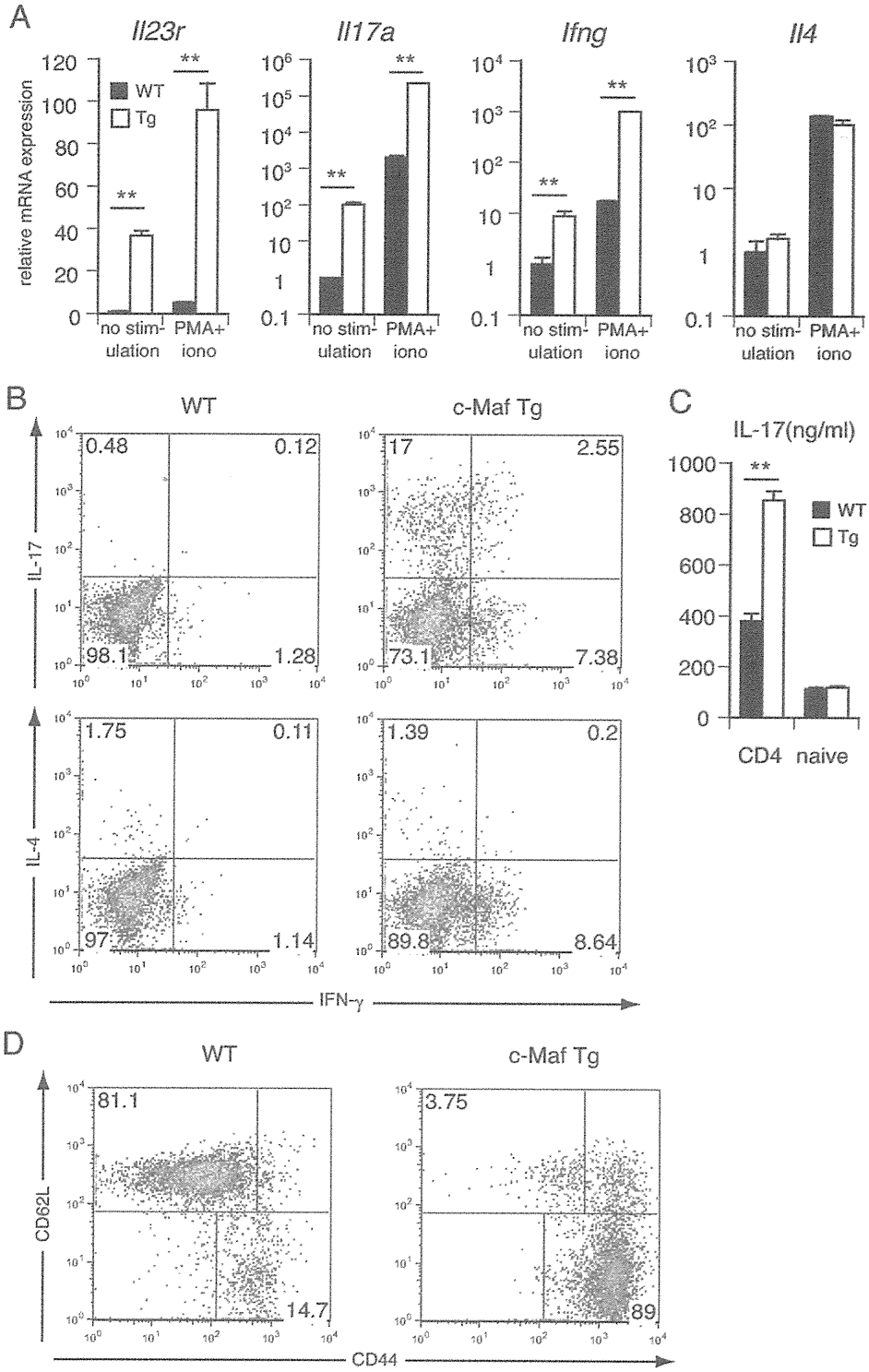

FIGURE 3. ***Ex vivo* gain-of-function analysis of c-Maf.** *A*, comparison between freshly isolated WT (*black bars*) and littermate c-Maf Tg (*white bars*) Th cells of the expression of Th differentiation markers. *B*, flow cytometric analysis of Th cells from c-Maf Tg and littermate WT mice. c-Maf Tg Th cells express more IL-17 and IFN-γ, but not IL-4, than control cells. *C*, IL-17 production from WT (*black bars*) and c-Maf Tg (*white bars*) Th cells or CD62L^{high} naive Th cells stimulated *in vitro* under Th17 differentiation condition for 2 days. IL-17 released into the culture supernatant was detected by ELISA. *D*, flow cytometric analysis of splenocytes from WT and c-Maf Tg mice gated on CD4$^+$ population. Single-cell suspensions of splenocytes were stained with anti-CD4-FITC, anti-CD44-PE, and anti-CD62L-APC mAbs and analyzed by FACSCanto. 7-Amino-Actinomycin D was used to separate dead cells. Similar results were obtained in three independent experiments. **, $p < 0.01$.

Ex Vivo Analysis of c-Maf-deficient Th Cells—As c-Maf deficient mice are embryonic lethal, we generated bone marrow chimeras by injecting *Maf*$^{-/-}$ fetal liver cells containing hematopoietic stem cells into irradiated Rag-2-deficient mice. Six weeks later, the donor mice were sacrificed, and flow cytometric analysis of splenocytes was performed. The ratio of effector-

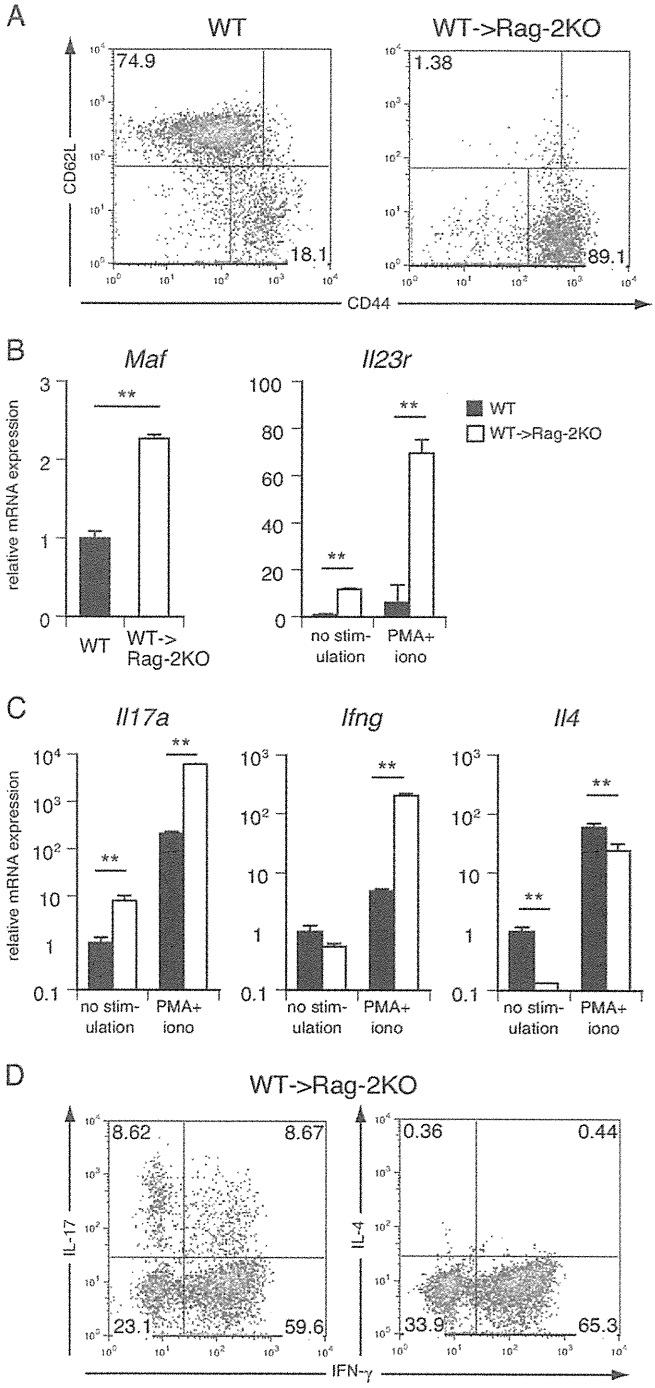

FIGURE 4. **Analysis of WT naive Th cells and memory Th cells derived from Rag-2-deficient mice transferred with WT Th cells.** *A*, flow cytometry of WT splenocytes and splenocytes from Rag-2-deficient mice transferred with WT Th cells (10^6/mouse) 4 weeks before analysis. An analysis similar to that shown in Fig. 3*D* was performed. Note that nearly 90% of the $CD4^+$ cells became $CD44^{high}$ $CD62L^{low}$, leaving only about 1% $CD44^{low}$ $CD62L^{high}$ cells. *B* and *C*, qRT-PCR analysis of the expressions of *Maf* and *Il23r* in naive (*black bars*) and memory (*white bars*) Th cells (*B*) and those of *Il17a*, *Ifng*, and *Il4* (*C*). *D*, flow cytometric analysis of memory phenotype Th cells. IL-17-positive and IFN-γ-positive populations were evident, but IL-4-positive one was not. Data represent three independent experiments. *PMA*, phorbol 12-myristate 13-acetate; *iono*, ionomycin. **, $p < 0.01$.

memory phenotype Th cells ($CD62L^{low}$ $CD44^{high}$) was not significantly different from that of WT Th cells (data not shown). As $Maf^{-/-}$-naive Th cells were shown to have the capacity to differentiate into Th17 cells *in vitro* (28), we decided to analyze the memory-phenotype c-Maf-deficient Th cells by transferring sorted splenic Th cells to Rag-2-deficient mice as in the experiment whose results are shown in Fig. 4 (Fig. 5*A*). In 4 weeks, most of the transferred Th cells acquired an effector-memory phenotype, and these cells were analyzed by qRT-PCR for the expressions of cytokines and *Il23r*. As expected, *Il23r*, *Il17a*, and *Ifng* expression levels were significantly lower in these cells than in the control WT cells. The expression level of *Il21*, which was reported to be a transcriptional target of c-Maf, was also lower (Fig. 5*B*).

DISCUSSION

In this study, we performed transcriptome analysis during the course of Th differentiation and unexpectedly found that c-Maf, considered to be a Th2-type transcription factor, is more prominently induced in Th17 cells than in Th2 cell. Moreover, factor analysis using the data of Th1-, Th2- and Th17-conditioned cells on days 1 and 3 demonstrated that *Maf* is more closely related to *Rorc* than *Rora* is to *Rorc*, at least in terms of the expression profiles in Th cells. As both RORγ and RORα are considered to play essential roles in Th17 differentiation (16), it occurred to us that c-Maf may also play an important role in Th17 cells. Bauquet *et al.* reported that inducible T cell costimulator (ICOS) is important for the expression of c-Maf in the development of follicular T helper cells (Tfh cells) and Th17 cells (28). In our culture system, we did not use ICOS-ligand for Th-cell stimulation. Thus, it is obvious that c-Maf can be induced in an ICOS-independent manner, probably through Stat3 activation by IL-6 (24).

As shown in the factor analysis results (Fig. 1*B*), *Maf*, *Rorc* and *Rora* were all high in Factor 2 but low in Factor 1. In contrast, *Gata3*, which encodes the master regulator transcription factor of Th2 cells, was very high in Factor 1 but low in Factor 2, and so was *Stat5a*, which is implicated in Th2 differentiation (29, 30). From these data, we may safely call Factor 1 "a Th2-related factor" and Factor 2 "a Th17-related factor". Indeed, *Tbx21*, which encodes the master regulator of Th1 cells, T-bet, was not high in either Factor 1 or Factor 2 and was positioned near the coordinate origin. Thus, these transcription factor groups specific to Th1, Th2 and Th17 cells are separately placed on the two-dimensional space defined by Factors 1 and 2.

IL-23R, which is required for the expansion of Th17 cells, is among the candidates for the transcriptional targets of c-Maf. Indeed, the promoter analysis revealed that MARE located in the 5′-prime lesion of *Il23r* is important for the luciferase activity induced by c-Maf overexpression, indicating that IL-23R is a direct target of c-Maf (Fig. 2*C*). IL-21 (28) and IL-10 (31) have also recently been reported to be targets of c-Maf in the context of Th17 differentiation. The analysis of c-Maf Tg mice, however, demonstrated that the overexpression of c-Maf did not seem to accelerate the early stage of Th17 differentiation (Fig. 3*C*). This finding is consistent with that of Bauquet *et al.*, in which c-Maf-deficient Th cells were capable of producing IL-17, although at a lower level (28). Instead, the significant

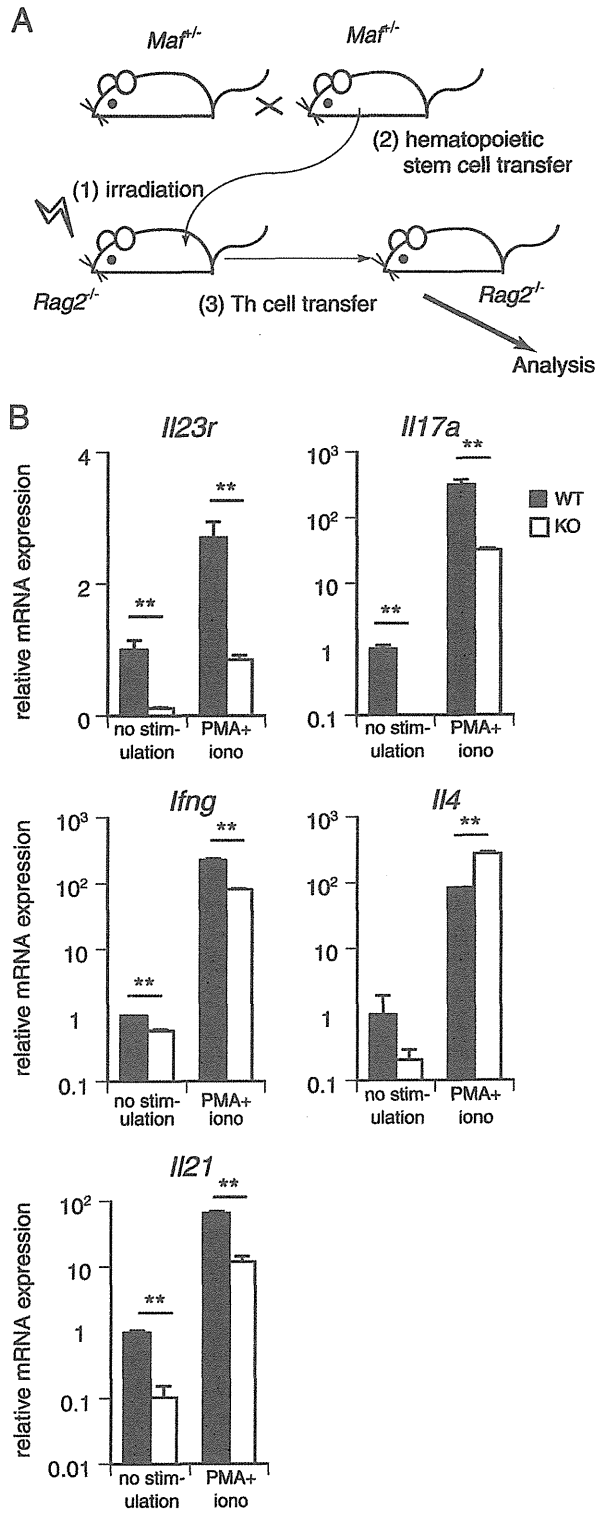

FIGURE 5. ***Ex vivo* loss-of-function analysis of c-Maf utilizing bone marrow chimera.** *A*, schematic diagram of producing bone marrow chimera and successive transfer of Th cells into Rag-2 knock-out mice. *B*, qRT-PCR analysis of the expressions of *Il23r*, *Il17a*, *Ifng*, *Il4*, and *Il21* in $Maf^{-/-}$ memory Th cells and control cells. Data represent three independent experiments. *PMA+ iono*, phorbol 12-myristate 13-acetate + ionomycin. **, $p < 0.01$.

deviation of Th cells toward the memory phenotype was observed in the Tg mice, suggesting that c-Maf may play a role in the development and/or maintenance of memory Th cells. The fact that WT mouse memory Th cells express higher mRNA levels of not only *Maf*, *Il23r* and *Il17a* but also *Ifng* than non-memory cells suggests that c-Maf indeed plays a role in memory Th17 and Th1 cells (Fig. 4*B* and *C*). In the earliest studies of Th cells and IL-17, it was memory Th cell that was shown to mainly produce the cytokine (32) particularly in response to IL-23 (33). It was not until the discovery of Th17 cells that these IL-17-producing cells were considered to be distinct from Th1 cells. Recently, however, Th cells that produce both IFN-γ and IL-17 have been gathering attention particularly in the context of inflammation, making the difference between Th1 and Th17 subsets less clear again (34–36). Although the relationship between memory Th cells and Th17 cells differentiated *in vitro* seems to be close in that both subsets express IL-23R, we have yet to determine whether Th17 cells differentiated *in vitro* are indeed the precursors of memory Th cells *in vivo*. If that is the case, c-Maf, which is expressed highly in both *de novo* Th17 cells and memory Th cell, may be a transcription factor that mediates the differentiation of the former into the latter.

In regard to this point, it is interesting that an IFN-γ/IL-17 double-positive population was evident in memory phenotype Th cells (Fig. 4*D*), which was not so apparent in Maf Tg cells. It is likely that the forced expression of c-Maf is sufficient for the expression of surface markers of memory Th cells, but not sufficient for the differentiation of IFN-γ/IL-17 double-positive Th cells.

The homeostatic expansion and induction of memory phenotype Th cells are important in a variety of clinical situations, such as during immunosuppressive therapy or chemotherapy. There is little doubt that the expansion of memory phenotype Th cells plays an important role in the defense against numerous pathogens, for example, those residing in the gut. At the same time, such expansion also bears the risk of autoinflammation, causing damage to self tissues. It has been shown that adoptive transfer of naive Th cells into lymphopenic hosts induces inflammatory bowel disease, which can be prevented by cotransfer of regulatory T (Treg) cells (37). Th1 response is implicated in the pathogenesis, whereas the role Th17 cells play in this disease model is still controversial (38). In either case, Treg cells seem to be essential for controlling the excessive response of homeostatically expanding Th cells.

It was unexpected that c-Maf Tg Th cells did not produce more IL-4 than WT cells (Fig. 3*A* and *B*), although c-Maf was reported to play an important role in IL-4 production (39). Consistently, the expression of *Il4* was not reduced in $Maf^{-/-}$ Th cells than in WT cells, either (Fig. 5*B*). These results may be explained by the fact that the Th1 cytokine IFN-γ strongly inhibits Th2 differentiation (40). Consistently, c-Maf Tg $CD62L^{low}$ Th cells caused Th1-mediated colitis in Rag-2-deficient mice whereas WT $CD62L^{low}$ Th cells did not (41). Thus, it is possible that the overexpression of c-Maf tips the balance of Th response toward Th1 rather than Th2 type under a neutral condition. In fact, c-Maf Tg Th cells produce more IL-4 than WT cells when cultured under a Th2 condition in the presence

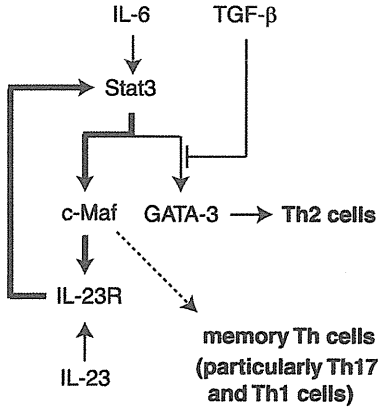

FIGURE 6. **Schematic diagram of Th cell differentiation.** IL-6 induces both c-Maf and GATA-3 via Stat3 phosphorylation and activation. GATA-3 expression can lead to Th2 differentiation, but this route is blocked in the presence of TGF-β, which inhibits GATA-3 expression. c-Maf induces IL-23R, and then IL-23 signaling activates Stat3, constituting a positive feedback loop (*boldface lines*). Although this loop does not seem to be essential to early Th17 differentiation, it may play an important role in the development and/or maintenance of memory Th cells, particularly memory Th17 cells.

of IL-4 and anti-IFN-γ antibody (in other words, in the absence of IFN-γ, data not shown). A schematic of Th cell differentiation is shown in Fig. 6; IL-6 induces c-Maf expression via Stat3 phosphorylation and is particularly important for the induction of IL-23R, which in turn augments Stat3 phosphorylation, constituting a novel positive feedback loop that leads to the differentiation of memory Th17 cells. On the other hand, TGF-β is likely involved in the inhibition of GATA-3 induction by IL-6, thereby blocking the pathway for Th cells to differentiate into Th2 cells.

c-Maf has also been implicated in the differentiation of other Th cell types, including Tfh cells (28) and regulatory type 1 (Tr1) cells (42). Our study indicates that this versatile transcription factor is also involved in the development and/or maintenance of memory Th (particularly Th17) cells. Clarification of the mechanisms of memory Th cell development in the context of c-Maf induction would be beneficial in the understanding of pathophysiology of various autoimmune inflammatory diseases.

Acknowledgments—We are grateful to S. Kano, M. Asagiri, H. J. Gober, and U. Sato for fruitful discussion and critical reading of the manuscript. We also thank Y. Meguro, M. Hamada, Y. Yamada, A. Kawano, and K. Watanabe for technical advice and assistance.

REFERENCES

1. Harrington, L. E., Hatton, R. D., Mangan, P. R., Turner, H., Murphy, T. L., Murphy, K. M., and Weaver, C. T. (2005) *Nat. Immunol.* **6,** 1123–1132
2. Park, H., Li, Z., Yang, X. O., Chang, S. H., Nurieva, R., Wang, Y. H., Wang, Y., Hood, L., Zhu, Z., Tian, Q., and Dong, C. (2005) *Nat. Immunol.* **6,** 1133–1141
3. Bettelli, E., Oukka, M., and Kuchroo, V. K. (2007) *Nat. Immunol.* **8,** 345–350
4. Steinman, L. (2007) *Nat. Med.* **13,** 139–145
5. Veldhoen, M., Hocking, R. J., Atkins, C. J., Locksley, R. M., and Stockinger, B. (2006) *Immunity* **24,** 179–189
6. Bettelli, E., Carrier, Y., Gao, W., Korn, T., Strom, T. B., Oukka, M., Weiner, H. L., and Kuchroo, V. K. (2006) *Nature* **441,** 235–238
7. Mangan, P. R., Harrington, L. E., O'Quinn, D. B., Helms, W. S., Bullard, D. C., Elson, C. O., Hatton, R. D., Wahl, S. M., Schoeb, T. R., and Weaver, C. T. (2006) *Nature* **441,** 231–234
8. Wilson, N. J., Boniface, K., Chan, J. R., McKenzie, B. S., Blumenschein, W. M., Mattson, J. D., Basham, B., Smith, K., Chen, T., Morel, F., Lecron, J. C., Kastelein, R. A., Cua, D. J., McClanahan, T. K., Bowman, E. P., and de Waal Malefyt, R. (2007) *Nat. Immunol.* **8,** 950–957
9. Manel, N., Unutmaz, D., and Littman, D. R. (2008) *Nat. Immunol.* **9,** 641–649
10. Volpe, E., Servant, N., Zollinger, R., Bogiatzi, S. I., Hupé, P., Barillot, E., and Soumelis, V. (2008) *Nat. Immunol.* **9,** 650–657
11. McGeachy, M. J., Bak-Jensen, K. S., Chen, Y., Tato, C. M., Blumenschein, W., McClanahan, T., and Cua, D. J. (2007) *Nat. Immunol.* **8,** 1390–1397
12. Ghoreschi, K., Laurence, A., Yang, X. P., Tato, C. M., McGeachy, M. J., Konkel, J. E., Ramos, H. L., Wei, L., Davidson, T. S., Bouladoux, N., Grainger, J. R., Chen, Q., Kanno, Y., Watford, W. T., Sun, H. W., Eberl, G., Shevach, E. M., Belkaid, Y., Cua, D. J., Chen, W., and O'Shea, J. J. (2010) *Nature* **467,** 967–971
13. Nishihara, M., Ogura, H., Ueda, N., Tsuruoka, M., Kitabayashi, C., Tsuji, F., Aono, H., Ishihara, K., Huseby, E., Betz, U. A., Murakami, M., and Hirano, T. (2007) *Int. Immunol.* **19,** 695–702
14. Yang, X. O., Panopoulos, A. D., Nurieva, R., Chang, S. H., Wang, D., Watowich, S. S., and Dong, C. (2007) *J. Biol. Chem.* **282,** 9358–9363
15. Ivanov, II, McKenzie, B. S., Zhou, L., Tadokoro, C. E., Lepelley, A., Lafaille, J. J., Cua, D. J., and Littman, D. R. (2006) *Cell* **126,** 1121–1133
16. Yang, X. O., Pappu, B. P., Nurieva, R., Akimzhanov, A., Kang, H. S., Chung, Y., Ma, L., Shah, B., Panopoulos, A. D., Schluns, K. S., Watowich, S. S., Tian, Q., Jetten, A. M., and Dong, C. (2008) *Immunity* **28,** 29–39
17. Morito, N., Yoh, K., Fujioka, Y., Nakano, T., Shimohata, H., Hashimoto, Y., Yamada, A., Maeda, A., Matsuno, F., Hata, H., Suzuki, A., Imagawa, S., Mitsuya, H., Esumi, H., Koyama, A., Yamamoto, M., Mori, N., and Takahashi, S. (2006) *Cancer Res.* **66,** 812–819
18. Imai, Y., Matsushima, Y., Sugimura, T., and Terada, M. (1991) *Nucleic Acids Res.* **19,** 2785
19. Sato, K., Hida, S., Takayanagi, H., Yokochi, T., Kayagaki, N., Takeda, K., Yagita, H., Okumura, K., Tanaka, N., Taniguchi, T., and Ogasawara, K. (2001) *Eur. J. Immunol.* **31,** 3138–3146
20. Kim, Y., Sato, K., Asagiri, M., Morita, I., Soma, K., and Takayanagi, H. (2005) *J. Biol. Chem.* **280,** 32905–32913
21. Kajihara, M., Sone, H., Amemiya, M., Katoh, Y., Isogai, M., Shimano, H., Yamada, N., and Takahashi, S. (2003) *Biochem. Biophys. Res. Commun.* **312,** 831–842
22. Ko, L. J., Yamamoto, M., Leonard, M. W., George, K. M., Ting, P., and Engel, J. D. (1991) *Mol. Cell Biol.* **11,** 2778–2784
23. Ho, I. C., Hodge, M. R., Rooney, J. W., and Glimcher, L. H. (1996) *Cell* **85,** 973–983
24. Yang, Y., Ochando, J., Yopp, A., Bromberg, J. S., and Ding, Y. (2005) *J. Immunol.* **174,** 2720–2729
25. Gorelik, L., Fields, P. E., and Flavell, R. A. (2000) *J. Immunol.* **165,** 4773–4777
26. Yamamoto, T., Kyo, M., Kamiya, T., Tanaka, T., Engel, J. D., Motohashi, H., and Yamamoto, M. (2006) *Genes Cells* **11,** 575–591
27. Min, B., Yamane, H., Hu-Li, J., and Paul, W. E. (2005) *J. Immunol.* **174,** 6039–6044
28. Bauquet, A. T., Jin, H., Paterson, A. M., Mitsdoerffer, M., Ho, I. C., Sharpe, A. H., and Kuchroo, V. K. (2009) *Nat. Immunol.* **10,** 167–175
29. Zhu, Y., Chen, L., Huang, Z., Alkan, S., Bunting, K. D., Wen, R., Wang, D., and Huang, H. (2004) *J. Immunol.* **173,** 2918–2922
30. Takatori, H., Nakajima, H., Hirose, K., Kagami, S., Tamachi, T., Suto, A., Suzuki, K., Saito, Y., and Iwamoto, I. (2005) *J. Immunol.* **174,** 3734–3740
31. Xu, J., Yang, Y., Qiu, G., Lal, G., Wu, Z., Levy, D. E., Ochando, J. C., Bromberg, J. S., and Ding, Y. (2009) *J. Immunol.* **182,** 6226–6236
32. Shin, H. C., Benbernou, N., Esnault, S., and Guenounou, M. (1999) *Cytokine* **11,** 257–266
33. Aggarwal, S., Ghilardi, N., Xie, M. H., de Sauvage, F. J., and Gurney, A. L. (2003) *J. Biol. Chem.* **278,** 1910–1914
34. Boniface, K., Blumenschein, W. M., Brovont-Porth, K., McGeachy, M. J., Basham, B., Desai, B., Pierce, R., McClanahan, T. K., Sadekova, S., and de

Waal Malefyt, R. (2010) *J. Immunol.* **185,** 679–687
35. Acosta-Rodriguez, E. V., Rivino, L., Geginat, J., Jarrossay, D., Gattorno, M., Lanzavecchia, A., Sallusto, F., and Napolitani, G. (2007) *Nat. Immunol.* **8,** 639–646
36. Kebir, H., Ifergan, I., Alvarez, J. I., Bernard, M., Poirier, J., Arbour, N., Duquette, P., and Prat, A. (2009) *Ann. Neurol.* **66,** 390–402
37. Izcue, A., Coombes, J. L., and Powrie, F. (2006) *Immunol. Rev.* **212,** 256–271
38. O'Connor, W., Jr., Kamanaka, M., Booth, C. J., Town, T., Nakae, S., Iwakura, Y., Kolls, J. K., and Flavell, R. A. (2009) *Nat. Immunol.* **10,** 603–609
39. Kim, J. I., Ho, I. C., Grusby, M. J., and Glimcher, L. H. (1999) *Immunity* **10,** 745–751
40. Gajewski, T. F., and Fitch, F. W. (1988) *J. Immunol.* **140,** 4245–4252
41. Weigmann, B., Nemetz, A., Becker, C., Schmidt, J., Strand, D., Lehr, H. A., Galle, P. R., Ho, I. C., and Neurath, M. F. (2004) *J. Immunol.* **173,** 3446–3455
42. Pot, C., Jin, H., Awasthi, A., Liu, S. M., Lai, C. Y., Madan, R., Sharpe, A. H., Karp, C. L., Miaw, S. C., Ho, I. C., and Kuchroo, V. K. (2009) *J. Immunol.* **183,** 797–801

European Journal of Immunology

Susceptibility loci for the defective foreign protein-induced tolerance in New Zealand Black mice: Implication of epistatic effects of *Fcgr2b* and *Slam* family genes

Takuma Fujii[1], Rong Hou[2], Aya Sato-Hayashizaki[2], Masaomi Obata[1], Mareki Ohtsuji[1], Kenichi Ikeda[1], Kenichi Mitsui[1], Yo Kodera[1], Toshikazu Shirai[2], Sachiko Hirose[2] and Hiroyuki Nishimura[1]

[1] Toin Human Science and Technology Center, Department of Biomedical Engineering, Toin University of Yokohama, Yokohama, Japan
[2] Department of Pathology, Juntendo University School of Medicine, Tokyo, Japan

In contrast to normal mice, autoimmune-prone New Zealand Black (NZB) mice are defective in susceptibility to tolerance induced by deaggregated bovine γ globulin (DBGG). To examine whether this defect is related to the loss of self-tolerance in autoimmunity, susceptibility loci for this defect were examined by genome-wide analysis using the F_2 intercross of nonautoimmune C57BL/6 (B6) and NZB mice. One NZB locus on the telomeric chromosome 1, designated *Dit* (*Defective immune tolerance*)-1, showed a highly significant linkage. This locus overlapped with a locus containing susceptibility genes for autoimmune disease, namely *Fcgr2b* and *Slam* family genes. To investigate the involvement of these genes in the defective tolerance to DBGG, we took advantage of two lines of *Fcgr2b*-deficient B6 congenic mice: one carries autoimmune-type, and the other carries B6-type, *Slam* family genes. Defective tolerance was observed only in *Fcgr2b*-deficient mice with autoimmune-type *Slam* family genes, indicating that epistatic effects of both genes are involved. Thus, common genetic mechanisms may underlie the defect in foreign protein antigen-induced tolerance and the loss of self-tolerance in NZB mouse-related autoimmune diseases.

Keywords: Autoimmune disease · IgG Fc Receptor · New Zealand Black mice · SLAM family · Tolerance

Supporting Information available online

See accompanying Commentary by Mitchison

Introduction

While there is diversity in immunological self-tolerant states, namely clonal deletion, anergy, or suppression of autoreactive lymphocytes, the mechanisms involved in the loss of self-tolerance may differ in different autoimmune diseases [1, 2]. Since Mitchison [3] proposed the immunological "paralysis" theory, foreign protein antigen-induced immune tolerance in vivo in mice has long been studied as a model of immunological self-tolerance (reviewed in [4]). It is well established that tolerance is inducible in adult mice by administering soluble foreign protein antigens such as bovine γ globulin (BGG) and human γ globulin (HGG) in a deaggregated form. Accumulating evidence has shown that, although both T-helper

Correspondence: Dr. Hiroyuki Nishimura
e-mail: nisimura@cc.toin.ac.jp

cells and B cells are involved in tolerance induction, the kinetics of tolerance induction differs between T and B cells, in that T-cell tolerance is achieved earlier after low-antigen doses, whereas tolerance in B cells requires more time and higher doses of tolerogens [5–7]. As the molecular mechanisms underlying these tolerance inductions have not been precisely identified, it remains elusive whether the same mechanisms are involved in the process of self-tolerance.

New Zealand Black (NZB) mice spontaneously produce autoantibodies reactive to erythrocytes and thymocytes, and autoimmune hemolytic anemia develops as these animals age (reviewed in [8]). They also produce IgM class anti-DNA antibodies and develop a mild form of immune complex-type glomerulonephritis later in life [8]. The interest in this strain as a systemic autoimmune disease model was given support by findings that, compared with findings in NZB mice, severe lupus nephritis associated with a high serum level of IgG autoantibodies develops spontaneously in the F_1 hybrid of NZB and nonautoimmune disease-prone New Zealand White (NZW) strains [9]. These findings clearly indicated that genes derived from both NZB and NZW mice contribute to this event. We previously found that the NZB locus, *Hig-1* (hyper IgG) in the telomeric region of chromosome 1, plays a pivotal role in the increased production of pathogenic IgG anti-DNA antibodies in (NZB × NZW)F_1 hybrid mice [10, 11]. *Hig-1* is tightly linked with *Fcgr2b*-encoding IgG Fc receptor IIB (FcγRIIB), a negative regulator of BCR-mediated activation signal in B cells [12, 13]. We found that *Fcgr2b* is polymorphic, and NZB *Fcgr2b* of autoimmune in nature. As the NZB-type *Fcgr2b* polymorphism has nucleotide deletions in the AP4-binding site in the promoter region, the FcγRIIB expression level on activated B cells is markedly suppressed, leading to B-cell activation and enhanced pathogenic autoantibody production [14].

In the vicinity of *Fcgr2b*, there exist polymorphic *Slam* family genes. Intensive congenic dissection studies showed that autoimmune-type *Slam* family genes play a significant role in the breakdown of self-tolerance and autoantibody production on a C57BL/6 mice (B6) genetic background [15]. As NZB mice have autoimmune-type *Slam* family genes, these genes are also suggested to contribute to the loss of self-reactive B-cell tolerance observed in autoimmune disease-prone NZB and (NZB x NZW)F_1 mice.

It has been a long time since NZB mice were found to be defective in their capacity to induce high-dose tolerance to deaggregated BGG (DBGG) [16, 17]. The defective tolerance in NZB mice was found to be an age-dependent phenomenon and preceded the onset of an autoimmune phenotypes in these mice [18]. Nevertheless, the cause–effect relationship between the defective tolerance to DBGG and the autoimmune disease of NZB mice remains unknown. In the present study, we mapped the loci responsible for the resistance to high-dose tolerance to DBGG in NZB mice in order to explore the relationship between the genetic predisposition for this defective high-dose tolerance and the autoantibody-mediated autoimmune disease.

Results

Defective immune tolerance induced by DBGG in NZB mice

We first examined whether DBGG-induced immune tolerance in our system is antigen specific. Three-month-old B6 mice were pretreated with PBS or DBGG, and immunized 1 wk later with BGG or OVA in the presence of CFA. After 1 wk, serum levels of antibodies against BGG and OVA were analyzed. Pretreatment with DBGG markedly downregulated the antibody response to BGG, but not to OVA (Fig. 1), indicating that DBGG-induced tolerance was antigen specific.

Figure 2 shows a comparison of serum levels of anti-BGG antibodies in normal B6, autoimmune-prone NZB, and (B6 × NZB)F_1 hybrid mice pretreated with DBGG or PBS and then immunized with BGG as in Fig. 1. Consistent with the earlier findings by others [16–18], NZB mice were defective in tolerance induction to DBGG, in contrast to the results in B6 mice. Tolerance induction in F_1 hybrid mice was intact as in the case of B6 mice. We then pretreated F_2 intercross mice ($n = 220$) with DBGG, immunized with BGG, and analyzed the levels of anti-BGG antibodies. Levels in F_2 intercross mice demonstrated a wide distribution, and 59% of the F_2 intercross mice showed impaired tolerance, when assuming that mice with anti-BGG antibody levels of less than 10^4 units were normal in terms of tolerance induction. These results suggest that the loci contributing to the defective tolerance are inherited in a recessive manner.

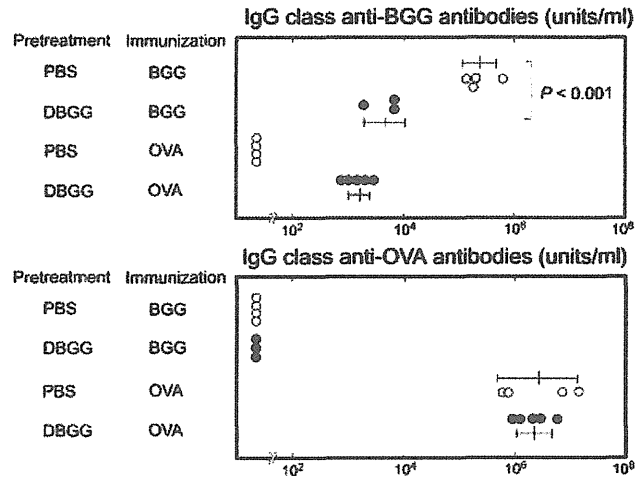

Figure 1. Antigen-specific immune tolerance induced by DBGG. Three-month-old female B6 mice were injected intraperitoneally with 10 mg of DBGG solution at days 0 and 7. Control groups of mice were injected with PBS. At day 14, mice were challenged either with BGG (250 μg) or with OVA (250 μg) emulsified in CFA in each of two hind footpads. Serum levels of IgG class anti-BGG and anti-OVA antibodies at day 21 were measured by ELISA. Pretreatment with DBGG downregulated the levels of antibodies specific to BGG but not to OVA. Closed circles and open circles show the levels of antibodies in mice pretreated with DBGG and with PBS respectively. Bars in each column represent means ± SD. The data are representative of three independent experiments.

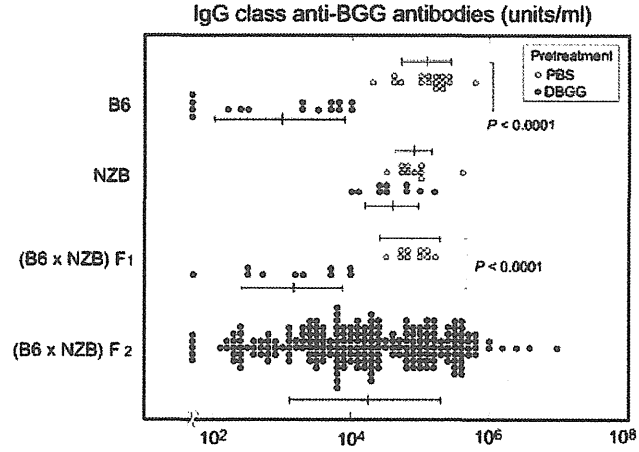

Figure 2. Serum levels of anti-BGG antibodies in B6, NZB, $(B6 \times NZB)F_1$, and $(B6 \times NZB)F_2$ intercross ($n = 220$) mice at day 21. These mice were pretreated with DBGG (closed circles) or with PBS (open circles), and were subsequently challenged with BGG plus CFA as in Fig. 1. Bars in each column represent means ± SD. Statistically significant differences between two groups pretreated with DBGG and PBS are shown with *p*-values in Mann–Whitney *U*-test.

Genome-wide mapping of loci for defective immune tolerance

$(B6 \times NZB)F_2$ intercross mice were genotyped for 130 polymorphic microsatellite markers distributed on all chromosomes except the sex chromosome (markers used are shown in Supporting Information), and quantitative trait loci (QTL) regulating the levels of anti-BGG antibodies shown in Fig. 2 were mapped. Linkage analysis identified two loci on NZB chromosomes 1 and 3 (Fig. 3). The peak LOD (logarithm of odds) score for the former was 7.20 at *D1Mit15*, and the peak LOD score for the latter was 4.38 at *D3Mit109*. On the basis of the criteria for genome-wide linkage studies [19], the locus on the telomeric region of chromosome 1 showed a highly significant linkage, and that on chromosome 3 showed a significant linkage. While the former showed a single peak, a broad interval on chromosome 3 showed significant linkage, suggesting that two or more genes in this interval may be involved. The susceptibility loci linked to *D1Mit15* and *D3Mit109* are provisionally designated as *Dit* (*Defective immune tolerance*)*-1* and *Dit-2* respectively, in which *Dit-2* represents a group of genes on chromosome 3. To examine the relationship between *Dit-1* and *Dit-2*, F_2 mice with B6/B6 or NZB/NZB homozygous genotype for each of *D1Mit15* and *D3Mit109* were selected and divided into four groups according to the combination of genotypes of *D1Mit15* and *D3Mit109*, and serum levels of anti-BGG antibodies were compared (Fig. 4). The results indicated that *Dit-1* and *Dit-2* showed an additive effect on the defective induction of tolerance.

Dit-1 is located in a region that overlaps with the reported autoimmune-susceptibility genes, namely, polymorphic *Fcgr2b* [11] and *Slam* family genes [15], suggesting that a common pathway plays a role in the defective immune tolerance to foreign protein and autoantibody production.

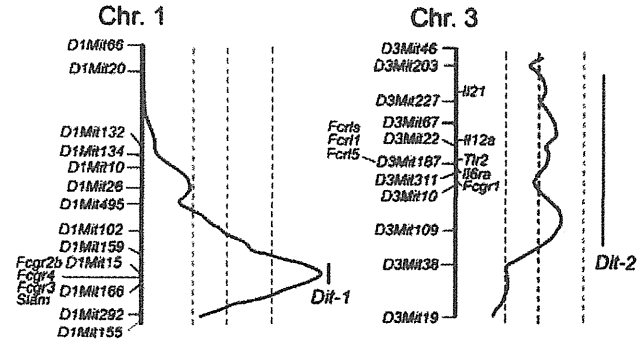

Figure 3. Loci regulating defective tolerance to DBGG obtained by genome-wide mapping in $(B6 \times NZB)F_2$ intercross mice ($n = 220$). The three bars on each figure show the minimum criteria for "highly significant" (LOD score = 4.8), "significant" (LOD score = 3.4), and "suggestive" (LOD score = 2.0) linkages. Two loci, *Dit-1* on the telomeric region of chromosome 1 and *Dit-2* on chromosome 3, showed "highly significant" and "significant" linkages respectively. The black bar for *Dit-1* and *Dit-2* represents the one-LOD support interval.

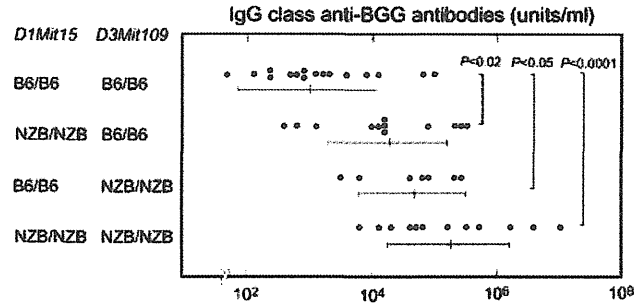

Figure 4. Comparison of serum levels of IgG anti-BGG antibodies after pretreatment with DBGG among four groups of $(B6 \times NZB)F_2$ intercross mice. Among 220 F_2 mice, mice with B6/B6 or NZB/NZB homozygous genotype for each of D1Mit15 and D3Mit109 were selected and divided into four groups according to the combination of genotypes of *D1Mit15* and D3Mit109. Bars in each column represent means ± SD. Statistically significant differences are shown with *p*-values in Scheffe's method.

Association of defective immune tolerance with autoantibody production in FcγRIIB-deficient mice

On the basis of the finding that the defective tolerance to DBGG in NZB mice is associated with the locus on chromosome 1 containing *Fcgr2b* and *Slam* family genes, we then analyzed the relationship of these genes. FcγRIIB is a negative regulator of BCR-mediated B-cell activation [12, 13] and FcγRIIB deficiency has been shown to induce autoantibody production on a B6 genetic background [20, 21]. Autoimmune-type *Slam* family genes were also reported to confer the predisposition for autoantibody production when introduced into mice with a B6 genetic background [15]. To explore the relationship between defective tolerance to DBGG and autoantibody production, we took advantage of two lines of FcγRIIB-deficient B6, established by selective backcrossing of the originally constructed FcγRIIB-deficient mice on a hybrid $(129 \times B6)F_1$ background into B6 mice [22]. Although both strains lack FcγRIIB expression, one carries 129 strain-derived autoimmune-type *Slam* family genes

and the other carries B6-derived *Slam* family genes (Table 1). The results showed that *Fcgr2b*-deficient mice with 129 *Slam* failed to exhibit tolerance to DBGG, whereas *Fcgr2b*-deficient mice with B6 *Slam* normally exhibited tolerance to DBGG (Fig. 5A). In addition, while these two strains did not develop anti-double-stranded (ds) DNA antibody production at 3 months of age, *Fcgr2b*-deficient mice with 129 *Slam*, but not *Fcgr2b*-deficient mice with B6 *Slam*, showed significantly high serum levels of anti-dsDNA antibodies at 6 months of age (Fig. 5B). As original B6 mice are susceptible to tolerance to DBGG and do not produce anti-dsDNA antibodies, these findings clearly show that the epistatic effect of *Fcgr2b* deficiency and autoimmune-type *Slam* family genes plays a pivotal role in both the defective tolerance induction to DBGG and autoantibody production.

Discussion

Autoimmune-prone NZB mice were defective in their abilities to acquire antigen-specific tolerance when injected with tolerogenic DBGG, in keeping with the previous studies [16, 17]. In the present study, we carried out genome-wide QTL analysis using (B6 × NZB)F_2 intercross mice to map the susceptibility loci for the defective tolerance to DBGG and two NZB loci, *Dit-1* and *Dit-2* on chromosomes 1 and 3 respectively, were identified. *Dit-1* showed a peak LOD score of 7.2, which exceeded the criterion of "highly significant" linkage in genome-wide studies [19] at marker locus *D1Mit15*. *Dit-2* showed a broad interval with significant linkage, suggesting that two or more candidate genes are present in this interval.

The microsatellite marker *D1Mit15* was also reported to be a marker of the cluster of autoimmune susceptibility loci, *Hig-1/Lbw7/Nba-2/Bxs3/Sle-1*, responsible for autoantibody production and/or lupus nephritis [11, 23–26]. These findings suggest that the defective tolerance to DBGG and autoantibody production share a common process regulated by *D1Mit15*-linked gene(s). Among the cluster of autoimmune susceptibility loci on the telomeric region of chromosome 1, *Hig-1* [11], *Lbw7* [23], and *Nba-2* [24] were NZB loci, whereas *Bxs3* [25] and *Sle1* [26] were BXSB and NZW loci. The precise causative gene(s) linked to these autoimmune susceptibility loci has been intensively studied by establishing interval congenic strains. Accumulating evidence obtained from these studies showed that the polymorphic *Fcgr2b* [27, 28] and *Slam* family genes [15, 27] are the most likely *D1Mit15*-linked candidate autoimmune susceptibility genes. There are other plausible candidate genes in the *D1Mit15*-linked region such as *Fcgr3* and *Fcgr4* (Fig. 3). Both mouse FcγRIII and FcγRIV have similarities to the human low-affinity IgG Fc receptor, FcγRIIIA, in genomic organization and sequence characteristics [12, 13]. As *Fcgr4* is not polymorphic between the two lines of FcγRIIB-deficient B6 mice used in the present study (Table 1), this gene may not be the candidate susceptibility gene. On the contrary, *Fcgr3* is polymorphic between the two lines of mice (Table 1). In humans, the significant association has been reported between the polymorphism of *FCGR3A* and the human systemic lupus erythematosus [29]. Thus, we cannot totally exclude the possible involvement of *Fcgr3* in the loss of self-tolerance and the defective tolerance to foreign proteins; however, there have been no reports indicating that the poly-

Table 1. Genotyping of the telomeric region of chromosome 1 in two lines of FcγRIIB-deficient B6 mice

Markers	Position (Mb)	FcγRIIB-deficient B6 mice with	
		129-derived *Slam*	B6-derived *Slam*
D1Mit187	115.45	B6	B6
D1Mit102	149.09	B6	129
D1Mit159	161.59	129	129
D1Mit15	170.28	129	129
Fcgr2b	172.89	Null	Null
Fcgr4	172.94	129	129
Fcgr3	172.98	129	B6
Slam family	173.48–174.40	129	B6
D1Mit359	179.21	129	B6
D1Mit221	187.04	B6	B6

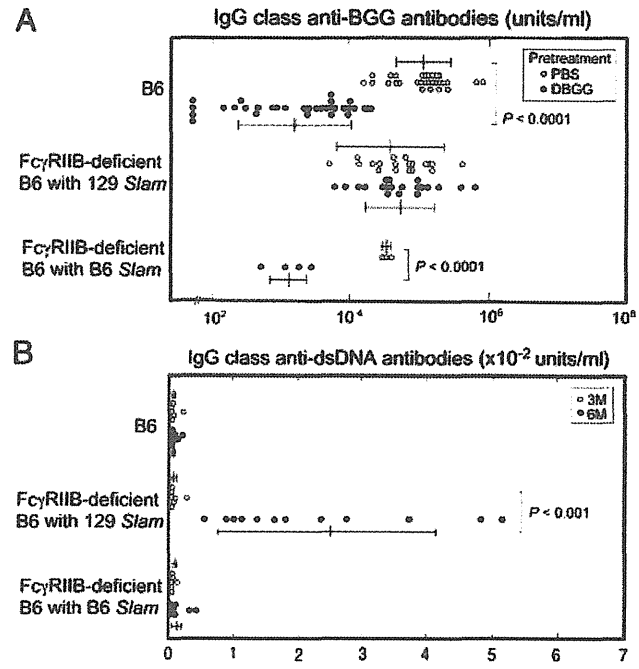

Figure 5. Defective immune tolerance and anti-dsDNA antibody production in FcγRIIB-deficient B6 mice with 129-derived *Slam* family genes. (A) B6, FcγRIIB-deficient B6 mice with 129-derived *Slam*, and FcγRIIB-deficient B6 mice with B6-derived *Slam* were tested for their abilities to exhibit tolerance by treatment with DBGG as in Fig. 1. Closed circles and open circles depict mice pretreated with DBGG and PBS respectively. (B) Comparison of serum levels of IgG anti-DNA antibodies among FcγRIIB-deficient B6 mice with 129-derived *Slam*, FcγRIIB-deficient B6 mice with B6-derived *Slam*, and B6 mice at 3 (open circles) and 6 months of age (closed circles). Bars in each column represent means ± SD. Statistically significant differences are shown with *p*-values in Mann–Whitney *U*-test. The data are representative of three independent experiments.

morphism of *Fcgr3* controls the immune regulation and/or the susceptibility to autoimmune disease in murine models.

Whitmer et al. [30] showed that FcγRIIB-deficient mice are normally susceptible to the induction of tolerance by deaggregated human γ globulin (DHGG). In the present study, we found that while FcγRIIB-deficient B6 mice carrying B6-type *Slam* were susceptible to tolerance induction by DBGG, as in the case of Whitmer's report [30], FcγRIIB-deficient mice carrying 129-type *Slam* showed defective induction of tolerance to DBGG. *Slam* family genes encode several molecules, such as *Cd244*, *Cd229*, *Cs1*, *Cd48*, *Cd160*, *Cd84*, and *Ly108* [31], and the 129 strain carries autoimmune-type, haplotype 2 *Slam* family genes, the same haplotype as that reported in the autoimmune-susceptible NZB, NZW, MRL, and BXSB strains [15]. Although the exact susceptibility gene(s) in multiple *Slam* family genes remains undetermined, *Ly108* may be a plausible candidate. It has been recently shown that, in addition to two splice isoforms, Ly108-1 and Ly108-2, *Ly108* produces the third isoform, Ly108-H1, which is absent in autoimmune-type *Ly108*, and that introduction of Ly108-H1-expressing transgene markedly suppresses autoimmunity by inhibiting T-cell proliferation in mice carrying autoimmune-type *Ly108* [32]. In any instance, SLAM family molecules are expressed in a wide variety of immune cells, and the homotypic and heterotypic interactions of these cell-surface molecules induce the phosphorylation of their cytoplasmic tails, allowing the subsequent binding of signaling molecules, namely, SLAM-associated protein (SAP) and EAT2, in the cytoplasmic tail. SAP is widely expressed in T cells and EAT2 is expressed in APCs. Thus, the polymorphism of *Slam* family genes may affect the function of T cells and APCs [31]. It has been well established that the tolerance induction by deaggregated γ-globulin develops at both T- and B-cell levels [5–7]. Since SLAM signal has been shown to modulate T-cell activation mediated by signals through TCR [31], it is feasible to speculate that the polymorphism of *Slam* family genes affects the strength of the TCR-mediated signal and the subsequent T-cell response against tolerogens. Komori et al. [33] reported that SAP deficiency ameliorated autoimmune disease in the MRL/*lpr* mouse model, which is characterized by the aberrant expansion of self-reactive T cells.

On the other hand, the deficient expression of FcγRIIB in NZB mice may intrinsically contribute to the defective tolerance induction at B-cell level, since FcγRIIB is a major negative regulator of B cells and has been shown to provide a distal peripheral checkpoint to limit the accumulation of autoreactive plasma cells, thereby maintaining tolerance [34]. NZB mice have autoimmune-type *Fcgr2b* polymorphism, shared by other autoimmune-prone strains of mice, such as BXSB, MRL, and NOD [11, 35]. Because of nucleotide deletions in the AP4-binding site in the *Fcgr2b* promoter region, the FcγRIIB expression level on activated B cells in these mice is ten times lower than the level in mice carrying a nonautoimmune B6-type polymorphism [11], leading to B-cell activation and enhanced pathogenic autoantibody production [14]. Xiang et al. [36] reported that FcγRIIB controls plasma cell persistence and apoptosis and that plasma cells from autoimmune-prone mice do not express FcγRIIB and are protected from apoptosis. Consistently, it has been shown that the deletion of the *Fcgr2b* gene renders mice highly susceptible to collagen-induced arthritis (CIA) with high levels of antibodies against collagen type II [37, 38], and that *Cia9*, one of the CIA susceptibility loci, is linked to the autoimmune-type *Fcgr2* in NOD mice [39]. The importance of autoimmune-type *Fcgr2b* in the pathogenesis of autoimmunity was further supported by our earlier finding that BXSB mice congenic for B6-type *Fcgr2b* showed no evidence of autoantibody production [28].

The present study strongly suggests that the combined effect of FcγRIIB deficiency and autoimmune-type *Slam* family genes is involved in both the defective tolerance to DBGG and the loss of self-tolerance in NZB mice. The concordant relationship between defective tolerance to DHGG and autoantibody production has been reported in the studies using the BXSB strain [40]. Because of the contribution of the *Y* chromosome-linked autoimmune acceleration (*Yaa*) mutation [41], BXSB male, but not female, mice develop severe lupus nephritis associated with high serum levels of anti-DNA autoantibodies. The *Yaa* mutation is expressed functionally in B cells [42] and duplication of the *Tlr7* gene has been proposed as an etiology for *Yaa*-mediated activation of self-reactive B cells [43–45]. Chu et al. [40] reported that while male BXSB mice were resistant, female mice were susceptible to the tolerance induction by DHGG. In this respect, it is to be noted that the BXSB and NZB strains share the same autoimmune-type polymorphic *Fcgr2b* and *Slam* family genes; nonetheless, tolerance to DHGG is normally induced in female BXSB mice, in contrast to the findings in NZB mice. These findings clearly indicate that additional genes, which are present in NZB and absent in BXSB female mice, are also involved in the defective tolerance induction. While in the BXSB strain, the *Yaa* mutation exerts this effect, such genes in the NZB strain remain unidentified. The current study suggests that one possible candidate is the NZB-derived *Dit-2*-linked gene(s). The interval overlapping with *Dit-2* on chromosome 3 has been reported to be involved in the upregulation of autoantibody production; however, the causative interval is derived from normal B10 or B6 mice [25, 46], thus it may differ from the NZB *Dit-2*. There are several potential candidate genes for *Dit-2*, such as *Il21*, *Il12a*, *Tlr2*, *Il6ra*, *Fcgr1*, and a group of genes for Fcγ receptor homologues, including *Fcrl1*, *Fcrl5*, and *Fcrls* (Fig. 3). It is worth noting that the region including *Fcgr1* and a group of genes for Fcγ receptor homologues on mouse chromosome 3 is syntenic with the 1q21–q22 region, which is linked with autoimmune susceptibility loci on human chromosome 1 [29]. Among these, *Fcrl5* codes for an Fcγ receptor homologue, FcRH3, with immunoreceptor tyrosine-based inhibitory motifs in the molecule [47], and has been shown to be transcribed in marginal zone B cells [48]. However, our preliminary study did not reveal any polymorphism between the NZB and the B6 strains in the coding sequence of *Fcrl5* (data not shown); thus, further studies are needed to identify the possible candidate genes for *Dit-2*.

The present linkage analysis suggests that common genetic mechanisms are operative for both the defect in tolerance induced by foreign proteins and the loss of self-tolerance in autoantibody-mediated autoimmune diseases. Our current study supports the notion that further studies on the mechanisms underlying the defective immune tolerance to DBGG at cellular/molecular levels in autoimmune disease-prone mice may extend

our understanding of the pathogenesis of antibody-mediated autoimmune diseases.

Materials and methods

Mice

NZB and B6 mice were obtained from Sankyo Laboratory Service (Tokyo, Japan) and were maintained in the animal-care facility at Toin University of Yokohama. Male NZB and female B6 mice were mated to obtain F_1 hybrids. Female (B6 × NZB)F_2-intercross mice ($n = 220$) were used for linkage studies. Two lines of FcγRIIB-deficient B6 mice were kindly provided by Dr. Toshiyuki Takai (Institute of Development, Aging and Cancer, Tohoku University, Japan) [22] and were bred in our animal facility. These strains were maintained under specified pathogen-free conditions. The study was reviewed and approved by the research ethics committee of Toin University of Yokohama.

Antigen

BGG (Sigma Chemicals, St. Louis, MO) was dissolved in PBS (pH 7.2) at 20 mg/mL and was sterilized using a 0.45 μ filter (Schleicher & Schuell GmbH, Dassel, Germany). Tolerogenic BGG was prepared as follows [18]. The BGG solution was ultracentrifuged at 100 000 × *g* for 2 h at 4°C using a SW41Ti rotor (Beckman Instruments, Palo Alto, CA). The top half of the BGG solution was collected and subjected to a second ultracentrifugation. After the second run, the top half of the DBGG solution was immediately used as tolerogenic BGG without storage. For immunization with CFA and for ELISA, BGG was further purified using a protein G Sepharose column (Pharmacia Biotech, Piscataway, NJ). Lyophilized ovalbumin, OVA (chicken egg albumin, grade VII) was obtained from Sigma Chemicals.

Induction of tolerance

On days 0 and 7, 3-month-old NZB, B6, (B6 × NZB)F_1 and (B6 × NZB)F_2-intercross mice were injected i.p. with tolerogenic DBGG (10 mg/mouse) dissolved in PBS. Control groups of mice were injected with PBS instead of DBGG. On day 14, mice were injected with BGG (250 μg) or OVA (250 μg) emulsified in CFA (Iatoron, Tokyo, Japan) in the hind footpads. On day 21, blood was obtained from the orbital venous plexus using a capillary tube and was allowed to clot at 4°C. Sera were stored at −20°C until analysis.

Antibody assay

Serum levels of IgG class anti-BGG antibodies were quantified using ELISA. ELISA plates were coated with 50 μL/well BGG and kept overnight at 4°C. Wells were blocked with 1% BSA in PBS at 37°C for 1 h, washed with PBS containing 0.05% Tween-20, and then incubated with 50 μL of serum samples serially diluted with PBS containing 1% BSA at 37°C for 1 h. The wells were then washed and incubated with 50 μL of goat anti-mouse IgG antibodies (1/5000) labeled with horseradish peroxidase (Zymed Laboratories, San Francisco, CA) in PBS containing 1% BSA at 37°C for 1 h. After washing, wells were developed with 2.8 mM *o*-phenylendiamine (Wako Chemicals, Osaka, Japan) in the presence of H_2O_2 (4.4 mM). The reaction was stopped with 2.5 N H_2SO_4 (50 μL), and absorbance at 490 nm was measured. A pool of sera obtained from B6 mice immunized with BGG was used as a standard serum pool containing one million units/mL of IgG class anti-BGG antibodies. Serum levels of anti-BGG antibodies are expressed in units, referring to a titration curve obtained by serial dilutions of the standard serum pool. Serum levels of IgG class anti-OVA antibodies were quantified using ELISA as for anti-BGG antibodies.

Serum levels of IgG anti-dsDNA antibodies were also measured using ELISA as described previously [14]. DNA was obtained from the calf thymus (Sigma Chemicals). DNA-binding activities are expressed in arbitrary units, referring to a standard curve obtained by the serial dilution of a standard serum pool from (NZB × NZW)F_1 mice over the age of 8 months, containing 1000 unit activities/mL.

Genotyping

Genomic DNA samples were extracted from tails. Polymorphism of microsatellite markers was analyzed by a modified version of the method described by Dietrich et al. [49]. Dye-labeled primer pairs were obtained from Applied Biosystems (Foster City, CA). PCR mixtures (7 μL) contained 120 nM each of forward and reverse primers, 2.5 mM of dNTP, 10 mM Tris-HCl (pH 8.3), 51 mM KCl, 1.5 mM $MgCl_2$, 4 μg/mL DNA, and 0.05 units/μL Taq polymerase (Invitrogen, Carlsbad, CA). The PCR amplifications were carried out using a GeneAmp 9700 PCR System (Applied Biosystems). The reaction consisted of initial denaturation at 94°C for 1 min, followed by 25 cycles of 94°C for 1 min, 56–58°C for 1.5 min, and 72°C for 10 min, and final extension at 72°C for 10 min. PCR products were analyzed using an ABI Prism 3700 DNA Analyzer (Applied Biosystems). A standard mixture of LIZ-labeled oligonucleotides (Applied Biosystems) was included in each run of the capillary electrophoresis. Sizes of the amplified microsatellite DNA were determined using GENESCAN and GENOTYPER software (Applied Biosystems).

For the genotyping of *Fcgr4* in two lines of FcγRIIB-deficient B6 mice, primers for PCR were designed to amplify the fragment containing *Fcgr4* SNPs of map position, Chr1:172948752, 172948763, 172948768, and 172948844, and PCR products were directly sequenced using the dideoxy chain termination method with *Taq* dye primer cycle sequencing kits (Applied Biosystems). Primers used were 5′-CAAACAACCAAACACACACAAA-3′ and 5′-ACCAAG GGGGATAGAACCAC-3′. Polymorphism of *Fcgr3* in B6-unique insertion and deletion sites of α-chain was determined by the length polymorphism of PCR product between 129 and B6, using 5′ primer,

5′-TCCATCTCTCTAGTCTGGTACC-3′ and 3′ primer, 5′-AAAA GTTGCTGCTGCCACC-3′. Polymorphisms of *Slam* families (*Cd229* and *Cd84*) were examined by single-strand conformational polymorphism. Primers for PCR were designed to amplify fragments encompassing the second exon of *Cd229* including amino acid position 130 and the second exon of *Cd84* including amino acid position 27. The 5′ and 3′ primers used were 5′-GCAGACTCAAAGTCAGC-GAAG-3′ and 5′-TGGTGAGGATAACATTCTTTTGG-3′ for *Cd229*, and 5′-AAAACAATTCAACAGTGTGATGG-3′ and 5′-AAGTCCAGGCAATG TTGTCA-3′ for *Cd84*. PCR products were denatured at 98°C for 10 min, loaded on an 15% polyacrylamide gel, and run in 0.5 × TBE employing a constant-temperature control system (AB-1600 and AE-6370, ATTO, Tokyo, Japan) at 17°C under a constant current of 20 mA/gel for 2 h. Single-stranded DNA fragments in the gel were visualized by silver staining (Daiichi Pure Chemicals, Tokyo, Japan).

Data analysis

Genomic interval mapping of QTL regulating the titers of antibodies in sera was performed using Map Manager software [50]. The criteria for the statistical significance of the linkage in genome-wide mapping [19] were empirically determined by permutation test using a program provided with the Map Manager package. The statistical variance analysis was done by Scheffe's method. Statistical analysis for the differences in antibody titers was carried out using Mann–Whitney *U*-test.

Acknowledgements: The authors thank Noriko Isoyama and Atsuko Kusano for the management of the mouse colonies and Noriko Iida for technical assistance. This work was supported in part by a Grant-in-Aid for Scientific Research (C) from the Ministry of Education, Culture, Sports, Science and Technology, Japan, a Grant-in-Aid (S0991013) from the Ministry of Education, Culture, Sports, Science and Technology, Japan, for the Foundation of Strategic Research Projects in Private Universities, and the Science Research Promotion Fund from the Promotion and Mutual Aid Corporation for Private Schools of Japan.

Conflict of interest: The authors declare no financial or commercial conflict of interest.

References

1 **Goodnow, C. C., Sprent, J., Fazekas de St Groth, B. and Vinuesa, C. G.,** Cellular and genetic mechanisms of self tolerance and autoimmunity. *Nature* 2005. **435**: 590–597.

2 **Kronenberg, M. and Rudensky, A.,** Regulation of immunity by self-reactive T cells. *Nature* 2005. **435**: 598–604.

3 **Mitchison, N. A.,** Induction of immunological paralysis in two zones of dosage. *Proc. R Soc. Lond. B Biol. Sci.* 1964. **161**: 275–292.

4 **Weigle, W. O.,** Immunological unresponsiveness. *Adv. Immunol.* 1973. **16**: 61–122.

5 **Dresser, D. W.,** Specific inhibition of antibody production. II. Paralysis induced in adult mice by small quantities of protein antigen. *Immunology* 1962. **5**: 378–388.

6 **Chiller, J. M., Habicht, G. S. and Weigle, W. O.,** Cellular sites of immunologic unresponsiveness. *Proc. Natl. Acad. Sci. USA* 1970. **65**: 551–556.

7 **Chiller, J. M. and Weigle, W. O.,** Cellular events during induction of immunologic unresponsiveness in adult mice. *J. Immunol.* 1971. **106**: 1633–1653.

8 **Shirai, T., Hirose, S., Okada, T. and Nishimura, H.,** Immunology and immunopathology of the autoimmune disease of NZB and related mouse strains. In: **Rihova, B. and Vetvicka, V.** (Eds.), *Immunological Disorders in Mice*, CRC Press, Boca Raton, FL 1991. pp. 95–136.

9 **Helyer, B. J. and Howie, J. B.,** Renal disease associated with positive lupus erythematosus tests in a cross-bred strain of mice. *Nature* 1963. **197**: 197.

10 **Jiang, Y., Hirose, S., Sanokawa-Akakura, R., Abe, M., Mi, X., Li, N., Miura, Y. et al.,** Genetically determined aberrant down-regulation of FcγRIIB1 in germinal center B cells associated with hyper-IgG and IgG autoantibodies in murine systemic lupus erythematosus. *Int. Immunol.* 1999. **11**: 1685–1691.

11 **Jiang, Y., Hirose, S., Abe, M., Sanokawa-Akakura, R., Ohtsuji, M., Mi, X., Li, N. et al.,** Polymorphisms in IgG Fc receptor IIB regulatory regions associated with autoimmune susceptibility. *Immunogenetics* 2000. **51**: 429–435.

12 **Ravetch, J. V. and Kinet, J-P.,** Fc receptors. *Annu. Rev. Immunol.* 1991. **9**: 457–492.

13 **Nimmerjahn, F. and Ravetch, J. V.,** Fcγ receptors: old friends and new family members. *Immunity* 2006. **24**: 19–28.

14 **Xiu, Y., Nakamura, K., Abe, M., Li, N., Wen, X. S., Jiang, Y., Zhang, D. et al.,** Transcriptional regulation of *Fcgr2b* gene by polymorphic promoter region and its contribution to humoral immune responses. *J Immunol.* 2002. **169**: 4340–4346.

15 **Wandstrat, A. E., Nguyen, C., Limaye, N., Chan, A. Y., Subramanian, S., Tian, X. H., Yim, Y. S. et al.,** Association of extensive polymorphisms in the *SLAM/CD2* gene cluster with murine lupus. *Immunity* 2004. **21**: 769–780.

16 **Staples, P. J. and Talal, N.,** Relative inability to induce tolerance in adult NZB and NZB/NZW F1 mice. *J. Exp. Med.* 1969. **129**: 123–139.

17 **Laskin, C. A., Taurog, J. D., Smathers, P. A. and Steinberg, A. D.,** Studies of defective tolerance in murine lupus. *J. Immunol.* 1981. **127**: 1743–1747.

18 **Laskin, C. A., Smathers, P. A., Lieberman, R. and Steinberg, A. D.,** NZB cells actively interfere with the establishment of tolerance to BGG in radiation chimeras. *J. Immunol.* 1983. **131**: 1121–1125.

19 **Lander, E. and Kruglyak, L.,** Genetic dissection of complex traits: guidelines for interpreting and reporting linkage results. *Nat. Genet.* 1995. **11**: 241–247.

20 **Bolland, S. and Ravetch, J. V.,** Spontaneous autoimmune disease in FcγRIIB-deficient mice results from strain-specific epistasis. *Immunity* 2000. **13**: 277–285.

21 **Nimmerjahn, F. and Ravetch, J. V.,** Antibody-mediated modulation of immune responses. *Immunol. Rev.* 2010. **236**: 265–275.

22 **Takai, T., Ono, M., Hikida, M., Ohmori, H. and Ravetch, J. V.,** Augmented humoral and anaphylactic responses in FcγRII-deficient mice. *Nature* 1996. **379**: 346–349.

23 **Kono, D. H., Burlingame, R. W., Owens, D. G., Kuramochi, A., Balderas, R. S., Balomenos, D. and Theofilopoulos, A. N.,** Lupus susceptibility loci in New Zealand mice. *Proc. Natl. Acad. Sci. USA* 1994. **91**: 10168–10172.

24 **Vyse, T. J., Rozzo, S. J., Drake, C. G., Izui, S. and Kotzin, B. L.,** Control of multiple autoantibodies linked with a lupus nephritis susceptibility locus in New Zealand black mice. *J. Immunol.* 1997. **158**: 5566–5574.

